Title
Hysteresis Patterns of Watershed Nitrogen Retention and Loss Over the Past 50 years in United States Hydrological Basins

Journal
Global Biogeochemical Cycles, 35(4)

ISSN
0886-6236

Authors
Newcomer, Michelle E
Bouskill, Nicholas J
Wainwright, Haruko
et al.

Publication Date
2021-04-01

DOI
10.1029/2020gb006777

Peer reviewed

Hysteresis Patterns of Watershed Nitrogen Retention and Loss over the past 50 years in United States Hydrological Basins

*Michelle E. Newcomer[1], Nicholas J Bouskill[1], Haruko Wainwright[1], Taylor Maavara[2], Bhavna Arora[1], Erica R. Siirila-Woodburn[1], Dipankar Dwivedi[1], Kenneth H. Williams[1,3], Carl Steefel[1], Susan S. Hubbard[1]

[1]Lawrence Berkeley National Lab, Earth & Environmental Sciences Area

[2]Yale University, School of the Environment

[3]Rocky Mountain Biological Lab, Gothic, CO

*Corresponding author: M. Newcomer, mnewcomer@lbl.gov

Key Points:

- Declines in nitrogen (N) exports in 34% of CONUS stream gages coincide with increasing N deposition and increasing vegetation productivity
- Watershed N retention displays both unique hysteresis (recovery) patterns and one-way transitions to new states
- Atmospheric deposition and vegetation explain >45% of the variability in watershed N retention trends, land use trends explain <10%

Index Terms: Watershed, Nitrogen cycling, river chemistry, Carbon cycling

Keywords: Watersheds, Nitrogen dynamics, ecosystem variability, catchment scale nitrogen retention, watershed exports, watershed N hysteresis

Abstract

Patterns of watershed nitrogen (N) retention and loss are shaped by how watershed biogeochemical processes retain, biogeochemically transform, and lose incoming atmospheric deposition of N. Loss patterns represented by concentration, discharge, and their associated stream exports are important indicators of integrated watershed N retention behaviors. We examined continental U.S. (CONUS) scale N deposition (wet and dry atmospheric deposition), vegetation trends, and stream trends as potential indicators of watershed N-saturation and retention conditions, and how watershed N retention and losses vary over space and time. By synthesizing changes and modalities in watershed nitrogen loss patterns based on stream data from 2200 U.S. watersheds over a 50 year record, our work revealed two patterns of watershed N-retention and loss. One was a hysteresis pattern that reflects the integrated influence of hydrology, atmospheric inputs, land-use, stream temperature, elevation, and vegetation. The other pattern was a one-way transition to a new state. We found that regions with increasing atmospheric deposition and increasing vegetation health/biomass patterns have the highest N-retention capacity, become increasingly N-saturated over time, and are associated with the strongest declines in stream N exports—a pattern that is consistent across all land cover categories. We provide a conceptual model, validated at an unprecedented scale across the CONUS that links instream nitrogen signals to upstream mechanistic landscape processes. Our work can aid in the future interpretation of in-stream concentrations of DOC and DIN as

indicators of watershed N-retention status and *integrators* of watershed hydrobiogeochemical processes.

Plain Language Summary

Watershed conditions around the world are changing in response to human activities. Indicators of watershed conditions can be streamflow measurements, river chemistry, and landscape characteristics, such as vegetation productivity. In-stream nitrogen (N) concentrations or exports (flow delivering N downstream) is a potential indicator of watershed conditions because of its significant potential to exacerbate hypoxic conditions along coastal zones. Our work provides an updated conceptual model for understanding watershed N retention conditions in response to atmospheric deposition patterns and watershed mechanisms. In particular, we utilize the wealth of publically-available continental US scale stream data from the US Geological Survey to demonstrate how watersheds can respond, recover, or transition to a new steady-state following atmospheric N-deposition.

1.0 Introduction

Watershed stream concentrations of nitrogen (N) and carbon (C), and hydrological connectivity driving exports of N and C to coastal zones have been changing around the world. Changes in N and C concentrations and exports (concentration x discharge) are often linked to a variety of direct and indirect causes at watershed scales which relate to the degree to which watersheds can retain N (Aber et al., 1998; Bernal et al., 2012; Crawford et al., 2019; Musolff et al., 2016; Smith et al., 1987; Stoddard, 1994; Vuorenmaa et al., 2018). Recent studies indicate that N and C watershed exports have increasing and decreasing trajectories in different watersheds across the continental United States (CONUS) over the last 50 years (Driscoll et al., 2003; Hale et al., 2015; Oelsner et al., 2017; Oelsner & Stets, 2019; Shoda et al., 2019). To explain these trends, studies often point to ecosystems recovering from acidic deposition (Lawrence et al., 2020; Stoddard et al., 1999), recovery from atmospheric N-deposition (Eshleman et al., 2013; Kothawala et al., 2011), watershed management (J. C. Murphy & Sprague, 2019), and agricultural practices (Renwick et al., 2018; Van Meter & Basu, 2015). Because the watershed ecological and biogeochemical characteristics controlling N and C retention, cycling, and loss are a non-linear function of N-deposition, many diverse hypotheses exist to explain trends of in-stream N and C conditions and exports and associated watershed N-retention (Aber et al., 1998; Bernhardt et al., 2005; Guo et al., 2019; Marinos et al., 2018; Stoddard, 1994). Despite the many existing studies examining controls on watershed N retention and loss at regional scales, a comprehensive analysis examining the co-occurrence of watershed N-retention and stream loss patterns has yet to emerge.

An important anthropogenic process directly linked to in-stream concentrations of N and C is atmospheric N-deposition. Around the world, atmospheric deposition of N has increased since the industrial revolution from fossil fuel combustion and fertilizer application (Pinder et al., 2012). Despite regulations on air pollution that have led to declining atmospheric N-deposition trends in some regions (Li et al., 2016), long term N-addition to watersheds via the atmosphere has significantly altered N-retention within watersheds. Specifically, N-retention capacity is the ability to retain or recycle N within the watershed. Retention is balanced by storage and biogeochemical cycling mechanisms that determine release of N which is exported via streams (Stoddard, 1994). N-saturation is a condition whereby N-inputs exceed the biogeochemical retention capacity of the system (watershed bioreactor capacity) to cycle, store, or retain N within living biomass (plants or microbes) or abiotic ecosystem components (e.g. soils). Once N-saturated conditions are reached, variable rates of C and N release to streams can occur (Pardo et al., 2011). The role of N-deposition on watershed retention of N and release to streams is an ongoing area of research complicated by both terrestrial and aquatic mechanisms.

Indeed, much of the debate over whether stream N is a function of atmospheric N deposition is centered on the degree to which watersheds can either retain and release N through biotic and abiotic factors (Aber et al., 2003; Lovett et al., 2000; Stoddard, 1994). Foundational nitrogen studies have hypothesized that alleviation of nitrogen limitation in soils have led to increased nitrate mobility, positive effects on vegetation productivity (Aber et al., 1998), and subsequent mobilization of nitrogen to streams (Stoddard, 1994). Once inputs surpass biological demand, the watershed may become N-saturated, and additional supply may lead to vegetation mortality through decreased cation availability (Lucas et al., 2011; Shultz et al., 2018), enhancing N transport through nitrification and mineralization. Observations of decadal declines in N concentrations and exports in streams despite increased N-deposition have confounded many of these foundational ideas (Goodale et al., 2003; Lucas et al., 2016). More recently however, significant reductions of atmospheric N deposition in some regions have reinvigorated research around this topic because of the opportunity afforded by this natural experiment to test these hypotheses (Eshleman et al., 2013).

Observations of trends in watershed N and C exports and concentration in streams have been proposed as potential indicators of watershed N-retention status because stream exports relate to landscape release patterns as indirect measurements of those same processes (Goodale et al., 2005). An extensive body of research has examined such stream measurements at regional-scales. Multi-decadal trends in surface water solute chemistry and export of dissolved organic carbon (DOC) and dissolved inorganic nitrogen (DIN) have been identified as a function of watershed characteristics, climate, and anthropogenic factors (Ballard et al., 2019; Bellmore et al., 2018; Boyer et al., 2006; Moatar et al., 2017; Musolff et al., 2015; Oelsner & Stets, 2019; Shoda et al., 2019; Stoddard et al., 1999; Zarnetske et al., 2018). Many studies have examined the role of atmospheric N-deposition in determining watershed N exports (Driscoll et al., 2003; Monteith et al., 2007; Musolff et al., 2017; Stoddard et al., 1999, 2016), however, the role of changing atmospheric loading on watershed N retention is confounded by additional hydrobiogeochemical and landscape variables. These include geology, vegetation, soil characteristics, microbial community composition, land cover/land use, climate, wetland cover (e.g. (Aber et al., 2003; Bellmore et al., 2018; Boyer et al., 2006; Stoddard, 1994)), wildfire (Jensen et al., 2017; S. F. Murphy et al., 2015; Rhoades et al., 2018), and source contributions directly to streams through agriculture and wastewater inputs which can in many cases comprise the majority of streamflow (Rice & Westerhoff, 2017). Direct internal sources (agriculture and wastewater) bypass any potential for soil and landscape transformation but are still subject to internal river/hyporheic transformations. While we acknowledge that wastewater, agricultural, and nitrogen fixation inputs are potentially large (estimates range from 2-80 kg/hectare, 30-90% of N budgets (Boyer et al., 2002; Van Meter et al., 2017)), quantifying these contributions at the CONUS scale has not been done to our knowledge and thus we can only estimate the potential magnitude of these terms based on the difference between deposition and stream exports (Figure 1). Because atmospherically deposited N becomes integrated into a range of biotic and abiotic transformations and redox cycling before reaching the stream, stream DIN and DOC exports may either deviate from or mirror atmospheric deposition trends (Argerich et al., 2013; Bernal et al., 2012; Halliday et al., 2013; Lovett et al., 2000; Musolff et al., 2015; SanClements et al., 2018).

A suite of mechanistic biogeochemical controls in the landscape have been identified as factors relating watershed N-retention to stream exports. Addition of N on the landscape has been documented to impact the following mechanisms: soil microbial mineralization/immobilization, and abiotic immobilization (Goodale et al., 2005; Huntington, 2005; Lovett et al., 2018), biotic uptake (Goodale et al., 2005; Huntington, 2005; Yanai et al., 2013), declining organic matter decomposition (Bowden et al., 2019; Janssens et al., 2010), shifting soil C:N ratios (Groffman et al., 2018; Yanai et al., 2013) leading to specific thresholding behavior for N release to streams (Evans et al., 2006), and altered soil organic carbon composition (Bowden et al., 2019; Evans et al., 2006) including declines in rapidly cycling labile carbon pools (Cusack et al., 2011). In addition, complex internal soil mechanisms responding to increasing atmospheric CO_2 have been found to drive increased N retention and soil carbon cycling limiting stocks of labile organic carbon (Groffman et al., 2018; Hungate et al., 1997; Huntington, 2005).

Once N and C reach the stream, additional biogeochemical and physical mechanisms exist that impact stream exports. In-stream response to variable DOC lability (Groffman et al., 2018; O’Donnell et al., 2010) can impact in-stream and hyporheic denitrification (Goodale et al., 2005) tilting streams towards thermodynamic limitations (e.g. monomeric and polymeric carbon) rather than kinetic limitations (e.g. concentration) (Garayburu-Caruso et al., 2020; Stegen et al., 2018). The pool of C and N that reaches the stream is also determined by hydrological conditions that shift stream water from fast to slow flow paths (i.e. runoff and infiltration partitioning). Deeper flows can access more aged, microbially sourced carbon pools (e.g., nonaromatic compounds, which are mineralized at different rates, (Schwesig et al., 2003)), while more shallow flows access younger, terrestrially derived carbon from vegetation and soils (Barnes et al., 2018). Given that shifts in precipitation (snow to rain transitions, greater extreme rain events etc.) are expected to be the dominant driver of changes in partitioning of runoff and infiltration as primary sources of water to streams (difference between young versus older water), changes in hydrology are quite likely to affect flow paths and access to different sources of carbon with varying characteristics in composition and degradability. Regionally, even slightly dryer conditions or greater evapotranspiration can lead to deeper flow paths and longer subsurface water residence times providing access to legacy nitrogen sources which might increase watershed exports despite little to no change in discharge. Legacy nitrogen is a potentially confounding variable that may impact direct analysis of watershed retention (Van Meter et al., 2016; Van Meter & Basu, 2015). Some physical processes such as turbulence set an upper limit on N-uptake within benthic biolayers and hyporheic zones (Grant et al., 2018). We point the reader to additional background material within the Supplementary Text SA2.

Despite the complexities discussed above, conceptual models examining connections between soil, atmospheric, vegetation, and stream water trends as indicators of and responses to deposition conditions have significantly advanced understanding of watershed response to decadal atmospheric N addition. Such conceptual models have identified many trajectories for landscape evolution after decades of atmospheric N deposition—watersheds may either return to the initial state after the perturbation (hysteresis), or transition to a new stable state (one-way transition) (Aber et al., 1998; Lovett et al., 2018; Vitousek & Reiners, 1975). Hysteresis in this sense refers to the recovery of the watershed to the original state, but through a different path. More recent conceptual models include previously unrecognized mechanisms related to soil N re-accumulation and storage (Lovett et al., 2018; Lovett & Goodale, 2011), and loss of base cations within soil (Lawrence et al., 2020). Observations of decadal long stream N and C hysteresis patterns, driven in some cases by state shifts between interacting soil mycorrhizal, microbial and plant communities after N deposition declines, point to the potential for biotic and abiotic conditions within watersheds to either reach a new equilibrium state or display hysteresis under declining N-deposition (i.e. recovery) (Gilliam et al., 2019). While these recent studies have advanced new conceptual models at the regional scale, they have yet to be tested against CONUS scale trends relative to watershed inputs and outputs. New insights and conceptual models will be needed to frame these stream trends in the context of important watershed characteristics and the vast amount of aquatic and terrestrial data available (Figure 1).

Figure 1 provides a watershed hydrobiogeochemical budget for N-retention with relevant processes occurring from the bedrock through the canopy. The watershed is treated as a closed unit that receives external inputs and produces external exports. All other processes are considered internal biogeochemical cycles and sources/sinks because they occur within the watershed unit. Retention within this unit is defined as the difference between external inputs and exports whereby the relative magnitude and importance of all internal processes within this watershed bioreactor is equal to this difference. During the progressive stages of atmospheric deposition of N, watersheds have the capacity to retain N through various soil and vegetation sink terms, and biogeochemical processes leading to reduced C and N delivery to streams, and export patterns unique to the 'watershed retention' stage (left side of watershed). During the recessive stage of atmospheric deposition, 'watershed recovery' occurs from decreased atmospheric deposition loadings, and watersheds exhibit unique patterns of stream export in response to greater lateral movement of C and N from soils to streams (right side of watershed).

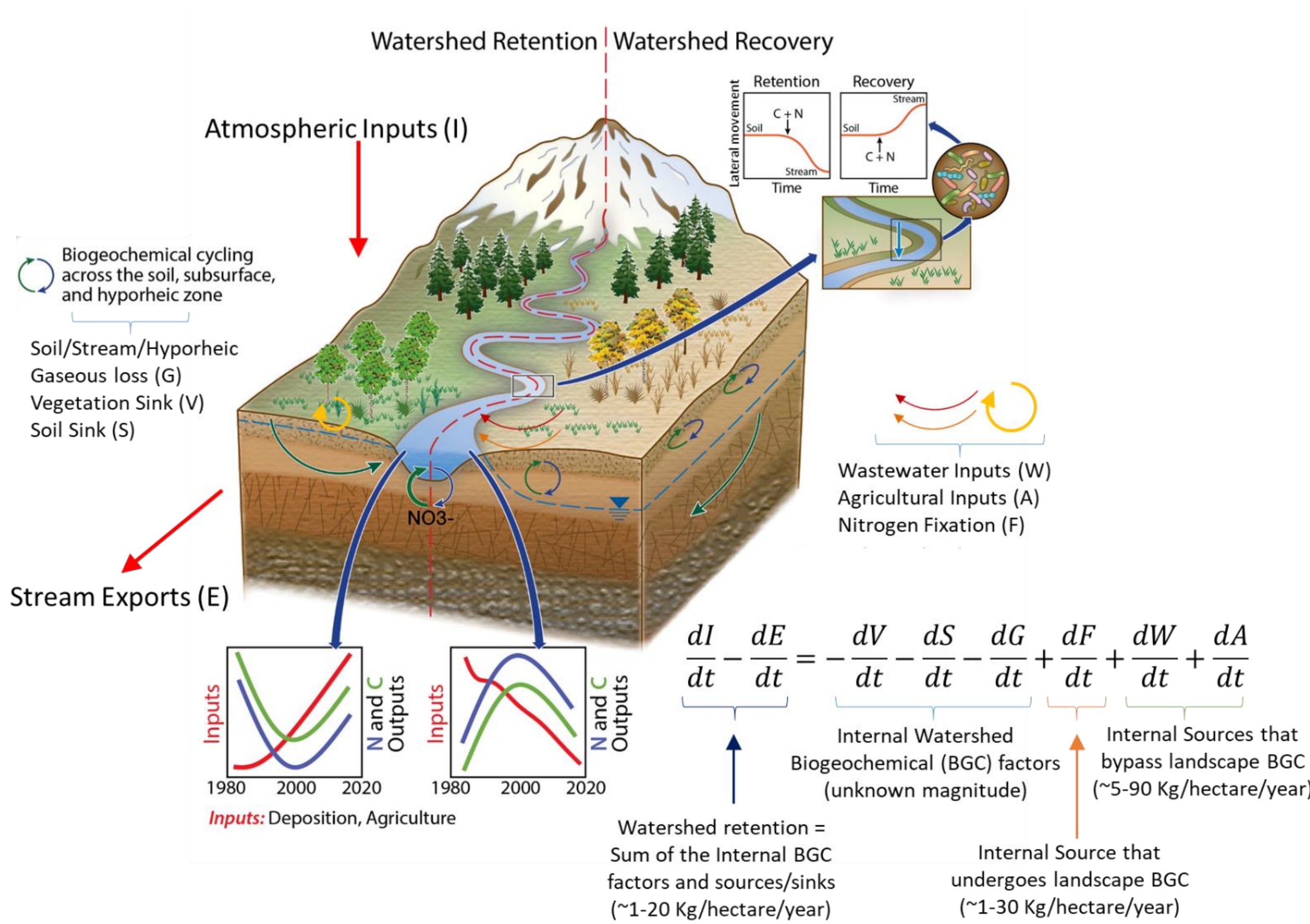

Figure 1: Hydro-biogeochemical processes occurring from bedrock to canopy and across elevation gradients influence the retention and transformation of atmospheric N deposition inputs (*I*), leading to distinct export signatures (*E*). Atmospheric input is the mass of wet and dry nitrogen deposition (kg hectare^{-1}), and export is the total stream load (mass flux) of nitrogen moved downstream relative to the total watershed area (kg hectare^{-1}). The watershed equation is modified from Lovett & Goodale (2011) where *dI/dt* is the atmospheric input rate (kg hectare^{-1} year^{-1}), and *dE/dt* is the stream export rate (kg hectare^{-1} year^{-1}). Internal biogeochemical factors are also listed: *dV/dt* is the rate of vegetation uptake, *dS/dt* is the soil sink rate, *dG/dt* is the soil and stream gaseous loss rate, *dF/dt* is the nitrogen fixation rate, *dW/dt* is the wastewater input

rate, and *dA/dt* is the agriculture input rate with similar units (kg hectare^{-1} year^{-1}). Lateral movement of N and C from the soils to the stream vary over time and as a function of N-saturation. Inputs and exports were evaluated at the yearly and seasonal time scales and the difference in inputs and exports is considered the sum of all internal biogeochemical processes and internal sources/sinks (i.e. storage or retention) where retention is then evaluated as a direct measure of the magnitude of internal processes/sources/sinks.

Using an updated conceptual model outlining N-dynamics (Figure 2, see section 2.1), our goal is to identify and quantify watershed N retention conditions, hysteresis patterns, and transitions across the CONUS using stream concentration and export indicators. The knowledge gaps related to watershed N-retention highlighted above motivate four research questions that we address: 1) Do watershed exports across CONUS divide neatly into the four conceptual categories (based on vegetation and atmospheric deposition) outlined in the text below, and in Figure 2? 2) How are in-stream N and C concentrations (*Cn*) and exports *(Ex)* changing, and how do these changes relate to discharge (*Qs*), and the categories in Figure 2 as potential covariates? 3) Do stream water chemical trends support the hypothesized groups of watershed N-retention and provide evidence for hysteresis patterns? 4) Can groups of changing atmospheric deposition and vegetation provide insight into hydro-biogeochemical processes controlling watershed export trends and watershed N-retention hysteresis or one-way transition patterns? We conduct this work over the CONUS scale to quantify and track where retention patterns are changing, and to provide conceptual guidance for large scale controlling factors on these trends including the role of deposition, vegetation, land-use, and in-stream conditions.

2.0 Materials and Methods

2.1 A Conceptual Model for Watershed N Retention and Loss

In the present study, we examine the degree to which CONUS scale atmospheric deposition patterns, vegetation trends, and stream trends can be potential indicators of watershed N-saturation, retention, and recovery conditions. We also examine how watershed N retention and losses vary over space and time. In this work we define watershed N losses as the stream export term, atmospheric deposition as the input term, and the difference between inputs and losses being equal to the internal soil, vegetative, fixation, and gaseous biogeochemical cycling terms (i.e. soil and aquatic denitrification) (Eshleman et al., 2013) as well as the unknown internal source terms (wastewater and agriculture). We do not directly analyze internal biogeochemical cycling and source/loss terms in this study (i.e. soil and aquatic denitrification as internal gaseous loss, agricultural and wastewater inputs), but we use knowledge of these mechanisms from many prior studies to help develop our conceptual model. Additionally, while these terms are quite important for the total watershed budget, they are difficult to quantify at CONUS and individual HUC2-HUC8 scales. Because of this, we hypothesize that the difference between external inputs and exports (atmospheric deposition and watershed export) is an important metric of the magnitude of internal biogeochemical processes and internal sources/sinks. Magnitudes of these terms are available in some literature sources (Boyer et al., 2002), however we do not have information on the magnitudes relative to the total HUC2-HUC8 watershed areas across CONUS for our study.

Our four stage hysteresis conceptual model of N-saturation and associated stream exports allows for reversal and recovery (i.e. hysteresis) or complete transition to a new steady state.

These patterns reflect the integrated signature of several factors, including atmospheric deposition trends, vegetation trends represented by remote-sensing measurements of normalized differenced vegetation index (NDVI), and stream conditions to explain trends (Lovett et al., 2000). With a reversal of N-deposition reported, we hypothesize this conceptual model will account for the wide variety of observed N concentration and export trends.

The four groups that are hypothesized to contribute to N and C export as a function of atmospheric N-deposition and vegetation NDVI trends are depicted in Figure 2:

- Group a, Retention: In those watersheds characterized by this group, N retention capacity is at its highest (can retain most of incoming N deposition). Watershed retention of incoming N deposition is close to 100% indicated by small watershed exports relative to deposition. This group is represented by locations where total atmospheric N deposition and vegetation health/biomass indices (represented by Normalized Difference Vegetation Index, NDVI) are increasing, leading to elevated N retention. Stream exports of N and C decline due to net immobilization in soils, high stream denitrification and in-stream assimilation from more thermodynamically favorable (more labile) carbon delivered to the stream and produced in the stream from photoautotrophs. These watersheds have not yet reached N-saturation loosely quantified by soil C/N molar ratios that are > 40 (Evans et al., 2006).
- Group b, Saturation: Retention capacity is still at its highest but approaching saturated conditions. Watershed retention of incoming N deposition is close to 100% indicated by small watershed exports relative to deposition, and some watersheds may indicate saturated conditions by showing declines in retention through increasing export trends. This group is represented by locations where total N-deposition continues to increase

over time, but vegetation biomass/productivity indices decline (negative NDVI trends). These watersheds generally show soil C/N ratios that are < 40. While N immobilization slows as biotic and abiotic stores become saturated, C and N delivery to streams is limited because landscape retention is still occurring. Moreover, continued stream denitrification leads to a lack of any obvious saturation or trend signal in river chemical parameters, accompanied by observations of predominant decreasing trends of riverine nitrogen, albeit with some increasing trends in DIN and labile DOC.

- Group c, Release: As watersheds undergo regional declines in atmospheric N deposition after experiencing periods of elevated atmospheric N deposition, vegetation biomass/productivity indices improve (positive NDVI trends), soils remain saturated in N relative to C, and N release from soils to streams continues. Even though leaching of N and organic matter to streams increases due to saturated conditions, immobilization and deeper N storage within soil horizons may continue but at a greatly declining rate depending on soil biotic/abiotic/microbial processes. Carbon begins to shift to a less thermodynamically favorable state (less labile) thereby limiting in-stream microbial denitrification, leading an increase in C export. In some locations it would be expected that stream exports of N increase because of the reduced capacity for soil N storage and from limited denitrification.
- Group d, Recovery: In the final stage of reversal from N-deposition, vegetation health indices show some signs of decline because of a return to N limiting conditions, soil provisions of N and C to the stream begin to increase as soil immobilization plateaus and C/N ratios rise above 40. Even though soil C and N delivery to streams continues,

continued decline of thermodynamically favorable carbon to streams limits denitrification potential and allows for continuous increases in stream exports of N.

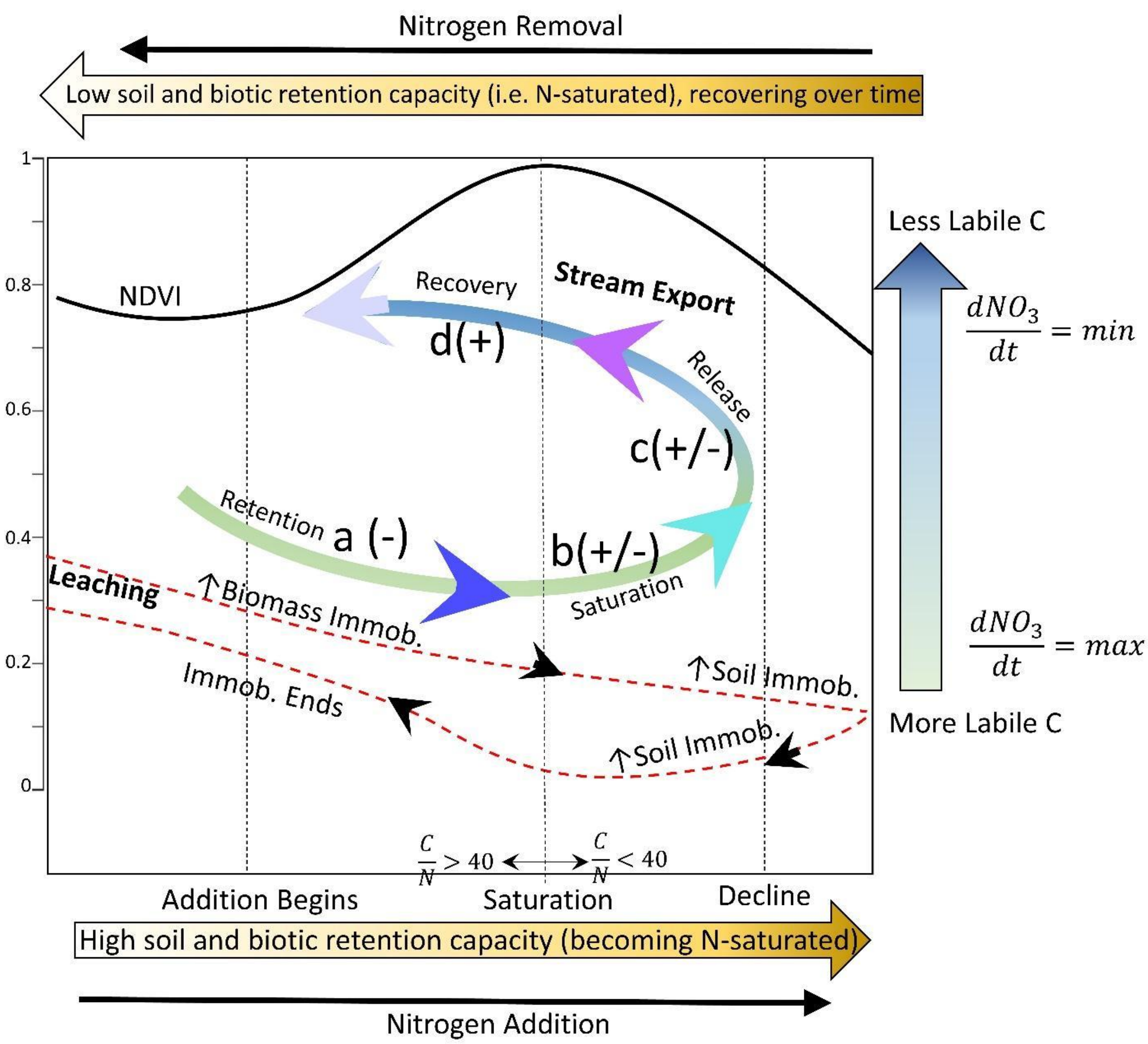

Figure 2: Our updated conceptual model of responses to N-saturation within watersheds showing the hysteresis pattern of N exports moving from retention to recovery. Figure modified from concepts described by Aber and Stoddard (Aber et al., 1998; Stoddard, 1994) and others (Gilliam

et al., 2019). The scale on the y-axis ranges from 0 to 1 to represent the magnitude and relative changes of each variable as a function of N addition (x-axis). The groupings a, b, c, and d, represent different stages on the hypothesized hysteresis curve of vegetation and NO_3 delivery response to N-deposition referenced in-text above. Group a should show a decline in stream exports (as indicated by '-'), Groups b and c show variable (+/-) stream exports depending on the other conditions, and Group d should show increases (+) in stream exports. Leaching, the process of soil delivery of N and C to streams by lateral movement is shown by the red dashed line and is represented as a function of soil and biomass immobilization. While immobilization occurs, leaching is reduced until immobilization ends. Denitrification rates (specifically related to the *dG/dt* term in Equation 1 and Figure 1) are represented by the arrow on the right side and decline from a maximum rate based on the most labile carbon available to a minimum rate as carbon becomes less labile.

To evaluate how watersheds across the US have responded to changes in depositional trends, we calculate decadal trends in stream concentrations and exports of C and N such as dissolved inorganic nitrogen (DIN) and dissolved organic carbon (DOC). We examine five variables of interest that are available at the CONUS scale and that represent controls on in-stream DIN concentrations and exports: net (wet+dry) atmospheric N-deposition, land-use and change, elevation, NDVI, and stream characteristics (temperature and DOC trends). We calculate trends using yearly and seasonal statistics across the last half-century of data acquired by the USGS and aggregate station trends using station and Hydrological Unit Code (HUC) scales across the CONUS. Statistics include trends in-stream concentrations (*Cn*), temperatures (*T*), discharge rates and volumes (*Qs*), bulk surface water mass exports (*Ex*), and bulk surface water area normalized mass exports or yields (*Ys*). We use the HUC scales as the watershed aggregating units.

2.2 Obtaining USGS Datasets and Calculating Exports

We analyzed in-stream C and N concentrations and discharge from USGS National Water Information System (NWIS) stations across the United States. This includes six different nitrogen parameters (Supplementary Table SA1), one carbon parameter, and temperature (USGS, 2016, 2018) (https://waterdata.usgs.gov/nwis). This big-data approach requires automated analysis to retrieve U.S. Geological streamflow, and concentration data from the long-term monitoring network NWIS using available USGS Web services (Read et al., 2017). Beginning with the watershed budget equation for retention from Figure 1 (Equation 1), we calculated a time-series of total mass exports past a stream station *Ex(t)* (kg $year^{-1}$) using the discharge *Qs(t)* and concentration *Cn(t)* time series by integrating from day 1 of each water year to day 365 for annual time series, and every 3 months for seasonal exports (Equation 2). The mass export is the multiplication of discharge *Qs(t)* (m^3 day^{-1}) and concentration *Cn(t)* (mg L^{-1} converted to kg m^{-3}) and summed for all daily time steps (Δt is for one day and for simplicity we represent this as dt in Equation 1 and Figure 1). Normalized exports (yields) were calculated by dividing the total mass export *Ex(t)* (kg $year^{-1}$ or Mg $year^{-1}$) by the drainage area (DA, km^2 or hectare) contributing to watershed yield at that particular station (kg km^{-2} $year^{-1}$ or Mg km^{-2} $year^{-1}$) (Equation 3). We converted all values to kg $hectare^{-1}$ $year^{-1}$, which is the unit associated with the atmospheric deposition time-series.

(1) $$\frac{dI}{dt} - \frac{dE}{dt} = -\frac{dV}{dt} - \frac{dS}{dt} - \frac{dG}{dt} + \frac{dF}{dt} + \frac{dW}{dt} + \frac{dA}{dt}$$

(2) Export=*Ex(t)*= $\sum_{day\ 1}^{day\ 365} Qs(t)Cn(t)dt$

(3) Normalized Exports (Yield)=*Ys(T)*=$\frac{\sum_{day\ 1}^{day\ 365} Qs(t)Cn(t)dt}{DA} = \frac{Export}{DA}$

Initial NWIS station selection was based on the criteria that a station was ‘maintained’ over time and not sampled just once. If a station had *any* available data for *Cn* and *Qs* defined as at least 20 observations of *any* measurements, the station was selected for the next step (see Supplementary Figures SA1-SA7 for data downloading methods and for station text files). We then developed a subset of stations with the criteria that available *Cn* data spanned across a minimum of 15 years, and contained at least 50 measurements of that *particular* parameter with associated daily *Qs* data. We required stations to have both *Qs* and *Cn* data available (see Supplementary Text SA3 for data retrieval methods and station files for each NWIS parameter). Since not all NWIS parameters are available at all stations, we used a different set of stations for each parameter. All NWIS data is retrievable through the R packages EGRET and dataRetrieval (Hirsch & De Cicco, 2015). Exports and Yields were calculated at the yearly and seasonal time-scale with daily *Qs*-*Cn* values requiring 365 data points for yearly calculations, and 90 for seasonal calculations. When *Cn* was not available for a particular day, we used a gap-filling approach described below (section 2.3). The final selection criteria considers the completeness of the station’s data across the different hydrologic unit code (HUC) 2-8 scales, and their distribution across elevation categories (Supplementary Table SA2, SA3, Figures SA1) (Seaber et al., 1987).

2.3 Gap-filling Datasets

To overcome the problem of sparse concentration and daily discharge data, discharge *Qs(t)* and concentration *Cn(t)* time-series statistics are used to gap-fill the *Cn* time-series using the USGS Weighted Regressions based on Trends, Discharge, and Seasonality (WRTDS) statistical method (Hirsch et al., 2010; Hirsch & De Cicco, 2015; Sinha & Michalak, 2016; Van Meter & Basu, 2017). Additionally, the averaging method (Kothawala et al., 2011; Lovett et al., 2000; Quilbé et al., 2006), and last-observation carried forward (LOCF) method (Moritz et al., 2015) were implemented for comparison to the WRTDS method, the detailed analysis and results of which are found in the Supplementary Information B-Additional Results. Gap-filling methods are necessary for the *Cn(t)* time-series because Equation 2 cannot be calculated for yearly or seasonal exports if *Cn* is not available at each daily time-step. Additional information regarding gap-filling datasets is available in Supplementary Text SA4.

2.4 Trend Detection and Statistical Significance

We calculated trends for the concentration time-series *Cn(t)*, export time-series *Ex(t)*, area normalized export time series (yields) *Ys(t)* and discharge time-series *Qs(t)*. We calculated trends for each nitrogen (N) and carbon (C) parameter using two techniques: 1) linear models to extract the slope (β) representing the trend, and 2) Mann-Kendall tests to extract the slope (β_{MK})

representing the trend (Forbes et al., 2019; Helsel & Hirsch, 2002). We analyzed a suite of statistics using the R statistical software for each time series (R Core Team, 2020).

To provide a robust approach to interpretation of trends (Renwick et al., 2018; Wasserstein & Lazar, 2016), statistical significance of trend tests and persistence of trends were obtained from three metrics: 1) the significance p-value for the linear slope (β) at the $p<0.05$ value, 2) the significance p-value for the Mann-Kendall trend parameter (β_{MK}) (Helsel & Hirsch, 2002) at the $p<0.05$ value, and 3) by calculating the persistence of trends using the Hurst Persistence analysis technique (Dwivedi & Mohanty, 2016; Hurst, 1951) using Hs=0.6 as the persistence cutoff value. Additional information regarding trend detection is available in Supplementary Text SA5.

2.5 Environmental Drivers of N retention

We directly compared yearly and seasonal trends in environmental drivers of interest to trends in surface water chemistry concentrations, exports and yields. Covariates of N-retention include net total (wet+dry) atmospheric deposition (TDEP, kg hectare^{-1}) (EPA CASTNET, 2019; NADP, 2018; Schwede & Lear, 2014), NDVI (Spruce et al., 2016), land cover/change (MRLC NLCD, 2020; Yang et al., 2018), stream conditions (changing temperature and DOC), elevation groups (Maurer, 2016; Maurer et al., 2004), and TDEP-NDVI grouping categories to represent distinct regions with unique watershed stages of N-saturation. We analyzed the dependent variable (N retention) with this potential set of explanatory variables using an ANOVA analysis to assess the percent of variability in N-retention explained by each variable. We used the Kruskall-Wallis test (K.W.) as a metric for statistical significance between groups of data such as *Ex* trends across elevation categories, or *Cn* trends across all NDVI-TDEP groups. All variable names, trend short-hand notation, and trend units used in this study are shown in Table 1. See additional details for the TDEP. NDVI, land-cover/change, and elevation products within Supplementary Text SA6.

Table 1: Potential covariates evaluated in the ANOVA analysis of Retention Capacity

Variable	Units	Symbol	Time-Series	Slope (β or βMK)	Slope Units
Concentration	mg/L	*C*	*C(t)*	ΔC	mg/L/year
Discharge	m^3/s	*Q*	*Q(t)*	ΔQ	m^3/year
Export	kg/day	*E*	*E(t)*	ΔE	kg/year or *Mg/year
Yield	$kg/km^2/day$	*Y*	*Y(t)*	ΔY	kg/ha/year or Mg/ha/year
Flow Normalized Concentration	mg/L	*FNC*	*FNC(t)*		mg/L/year
Flow Normalized Export	kg/day	*FNE*	*FNE(t)*		kg/year or Mg/year
Flow Normalized Yield	$kg/km^2/day$	*FNY*	*FNY(t)*		kg/ha/year or Mg/ha/year
Normalized Differenced Vegetation Index	unitless	*NDVI*	*NDVI(t)*	$\Delta NDVI$	"-"/year
Total Wet+Dry Nitrogen Deposition	kg/ha	*TDEP*	*TDEP(t)*	$\Delta TDEP$	kg/ha/year
Stream Temperature	Celsius	*Temp*	*T(t)*		Deg.Celcius/year
Elevation	m	*ELEV*			Categorical
Land-cover/change	-	*LC/LCC*	-		Categorical

* Mg is megagrams = 1E6 grams

From the total TDEP deposition and the total stream losses (stream yields *Y(t)*) per area, we calculated the watershed retention capacity by subtracting the yearly watershed yield *Y(t)* (kg hectare^{-1}) from the yearly TDEP depositional inputs (kg hectare^{-1}) (Equation 4) (Lovett et al., 2000). Though we do not directly analyze biogeochemical mechanisms and confounding factors within our study, we acknowledge that a critical insight from all the prior work is that biogeochemical cycling within the watershed is an important component to long-term stream exports than atmospheric N-deposition alone (Lovett et al., 2000; Lucas et al., 2016). Internal biogeochemical cycling terms for vegetation sinks (V), soil sinks (S), gaseous loss sinks (G), and fixation (F), agriculture (A), and wastewater (W) inputs (Figure 1) are unknown internal biogeochemical source/sink terms not accounted for in the retention equation, however the magnitude of influence of these terms can be estimated with the retention equation.

(4) Annual Retention Capacity = $\frac{Inputs - Exports}{Inputs} * 100$

2.6 Watershed Aggregation

Once station-based statistics, models, and trends were constructed, the slope values and the statistics were aggregated to the different hydrologic unit code (HUC) 2-8 scales. When aggregating trends from the station to the larger HUC2-HUC8 scales, we used two approaches:

Simple averaging: Simple-averaging is the arithmetic mean where all values have equal weight in the calculation. We used simple averaging of trends across all stations to get the aggregated HUC2-HUC8 trends, to map average trends in exports, concentrations, yields, and discharge. We evaluated the significance of these trends by counting the number of stations within each watershed that had statistically significant trends at $p<0.05$. Additionally, we averaged only statistically significant station trends across groups: TDEP-NDVI groups, elevation groups, and land cover.

Area-Weighted averaging: Area-weighted averaging is a method of aggregating values by applying weight to the values based on another variable. We calculated area-weighted averages by weighting the trend values using contributing drainage areas such that exports from larger contributing areas provide more weight to the average than exports from smaller contributing areas.

To aggregate the statistical significance from the station scale to the HUC 2-8 scale, we used a station thresholding approach to identify how many watersheds contain more than 50% of stations with statistically significant and directionally similar trends in exports and concentrations, or exports and discharge. We compared trends in station exports, concentrations, yields, and discharge and counted the number of stations showing statistically significant ($p<0.05$) and directionally similar trends (positive or negative) in these variables for every HUC2-HUC8 watershed. Because this CONUS 'big-data' approach requires a significant amount of computational capabilities, all data processing and analysis was performed on the LBNL NERSC supercomputer Cori. We used over 30000 core hours requiring over 500Gb of memory on the Cori 'Big-Memory' node and analyzed over 1Tb of data. All gap-filled CONUS datasets used in this study can be found on the public repository ESS-DIVE (https://doi.org/10.15485/1647366) (Newcomer et al., 2020). Additional watershed aggregation details can be found in the Supplementary Text SA7.

3.0 Results

Our results section is structured as follows: we first present results of the trend analysis for TDEP, NDVI, and in-stream parameters for DIN, DOC, and Temp related to our first and second research questions (section 3.1, 3.2, and 3.3). We then examine how watershed exports and watershed retention relate to the conceptualized TDEP-NDVI groups presented in Figure 2 to address our third and fourth research questions (section 3.4). Finally, we provide results examining potential controlling factors on watershed retention including land use and elevation, and describe the modalities of watershed retention hysteresis and one-way transition patterns (section 3.5 and 3.6).

3.1 TDEP-NDVI Grouping Classification

Considerable spatial variability in TDEP and NDVI trends is found across the CONUS (Figure 3). General patterns across a few HUC2 scales are highlighted. In HUC2 basin #10 (Missouri Basin), patterns of increasing NDVI and increasing TDEP (Group a) reflect the majority of HUC8 scale watersheds within the Missouri. Across the South Atlantic-Gulf Basin (HUC2 #03), increasing trends in NDVI are associated with decreases in TDEP (Group c). In the Ohio Basin (HUC2 #05), decreasing patterns of NDVI are observed with decreasing patterns in TDEP (Group d). Across the Pacific Northwest Basin (HUC2 #17), spatial variability in N-saturation groups are found with regions showing difference in TDEP and NDVI. Many HUC8 regions within the Pacific Northwest fall into Group b, representing increases in TDEP and declines in NDVI. Across the CONUS, 10.2% of HUC8 watersheds fall into Group a, 7.8% in Group b, 8.5% in Group c, and 8.9% in Group d. The other remaining 64% are not end-member groups, but rather fall between these end-member groups. We use the TDEP-NDVI groupings throughout the rest of the paper to facilitate interpretation of watershed N-losses and N-retention trends. TDEP-NDVI groups and their conceptualized role on in-stream trends are provided in Figure 2.

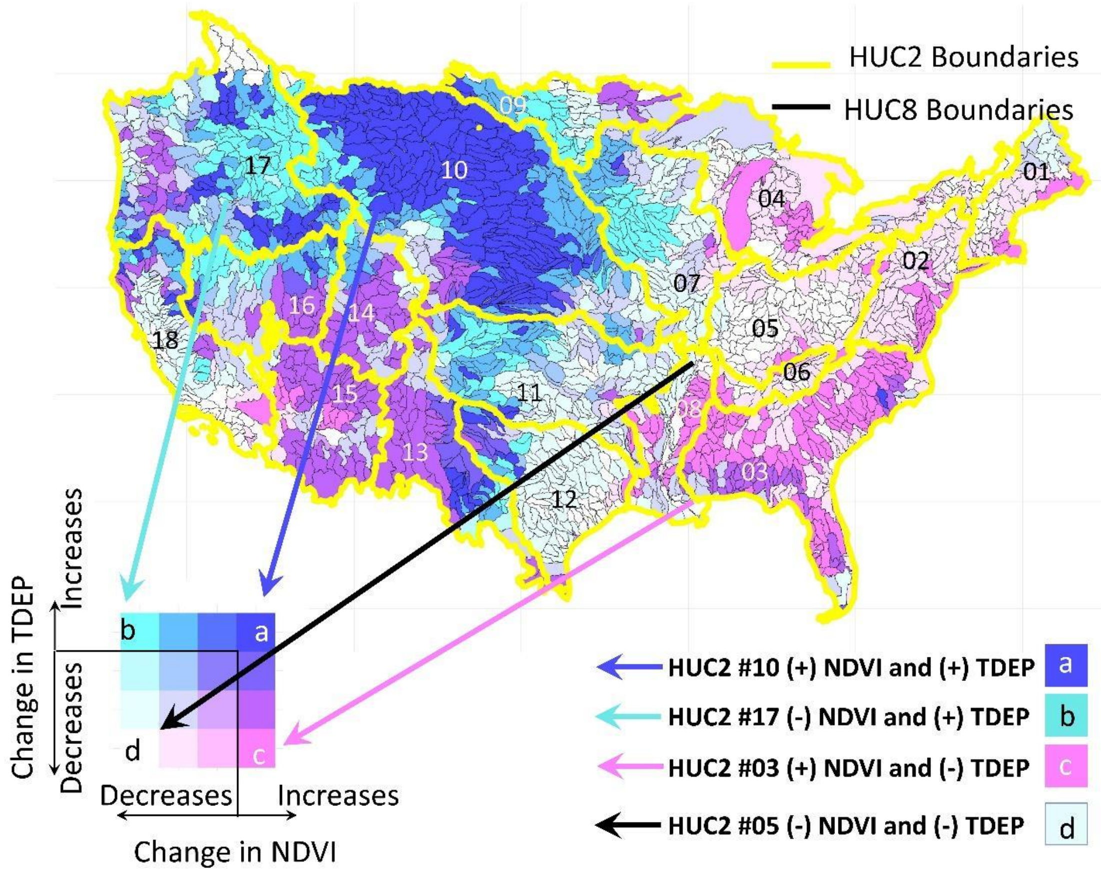

Figure 3: Groupings and directionality of vegetation and deposition change based on trends in TDEP (2000-2018) and NDVI (2000-2015). Groupings include: Group a) regions with increasing NDVI and increasing TDEP, Group b) regions with decreasing NDVI and increasing TDEP, Group c) regions with increasing NDVI and decreasing TDEP, and Group d) regions with decreasing NDVI and decreasing TDEP. HUC2 boundaries are shown by the yellow line with their corresponding HUC2 basin numbers. Groups a-d and their colors are used consistently throughout the rest of this paper and refer to the same groups illustrated in Figure 2 and defined in Section 2.1 describing the conceptual model.

3.2 Concentration Trends across US Basins

CONUS-wide DIN concentration trends across HUC4 watersheds shows wide-variability (Figure 4a). All means are calculated from stations with statistical significance as defined in the methods section. Across the CONUS, 36.5% of stations show statistically significant declining concentrations of DIN (-0.005 ± 0.004 mg/L/year), while 38.1% of stations show statistically significant increasing concentrations of DIN (+0.0082 ± 0.0092 mg/L/year). It is common for river chemistry datasets to have such large standard deviations because of interannual variability (i.e. (Strauss et al., 2004)). Similarly, across the CONUS we find increasing and decreasing trends in DOC concentrations for the different HUC2 and HUC4 basins from 1970-2020 (Figure 4b), however major gaps in DOC coverage occur across the CONUS. On average, 57.9% of HUC4 watersheds show statistically significant decreasing concentrations (-0.067 ± 0.049 mg/L/year), while 14.5% of HUC4 watersheds show statistically significant increasing concentrations (0.022 ± 0.027 mg/L/year). Temperature maps (Supplementary Figure SB1) and temperature statistics are also provided (Supplementary Table SB1).

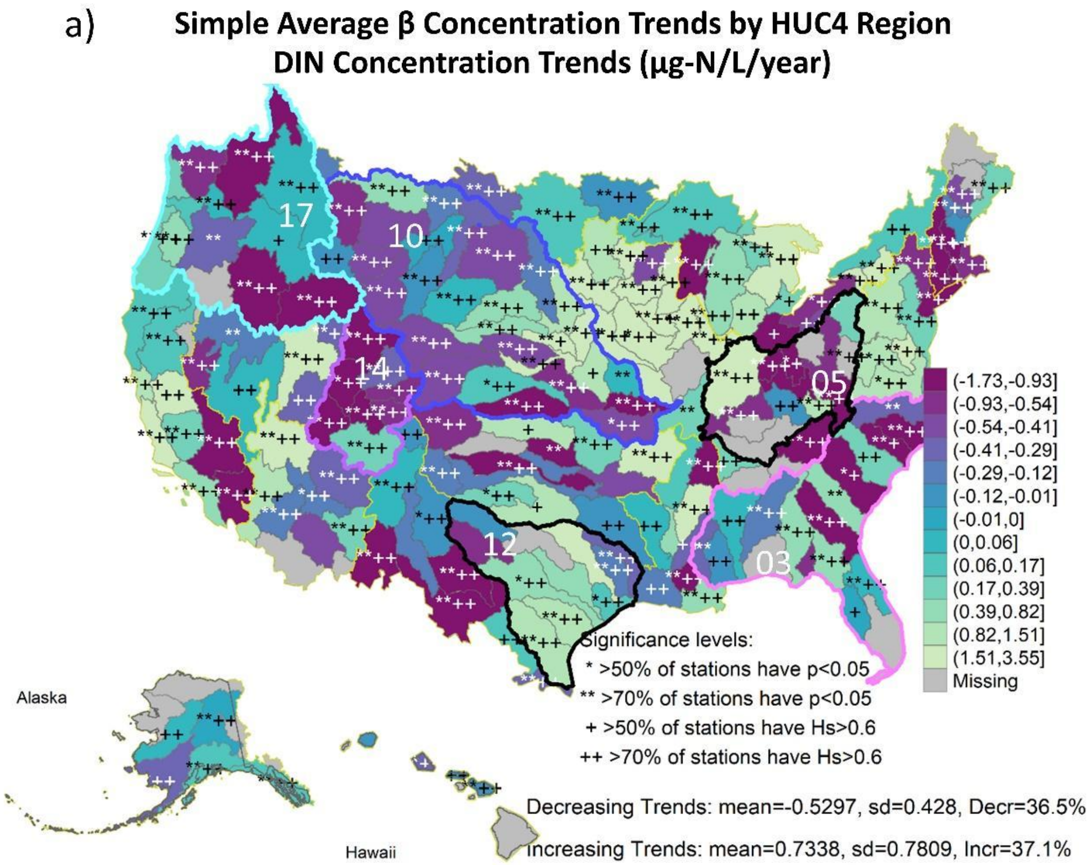
a)
Simple Average β Concentration Trends by HUC4 Region
DIN Concentration Trends (μg-N/L/year)
17
10
14
05
12
03
(-1.73,-0.93]
(-0.93,-0.54]
(-0.54,-0.41]
(-0.41,-0.29]
(-0.29,-0.12]
(-0.12,-0.01]
(-0.01,0]
(0,0.06]
(0.06,0.17]
(0.17,0.39]
(0.39,0.82]
(0.82,1.51]
(1.51,3.55]
Missing
Significance levels:
* >50% of stations have p<0.05
** >70% of stations have p<0.05
+ >50% of stations have Hs>0.6
++ >70% of stations have Hs>0.6
Alaska
Hawaii
Decreasing Trends: mean=-0.5297, sd=0.428, Decr=36.5%
Increasing Trends: mean=0.7338, sd=0.7809, Incr=37.1%

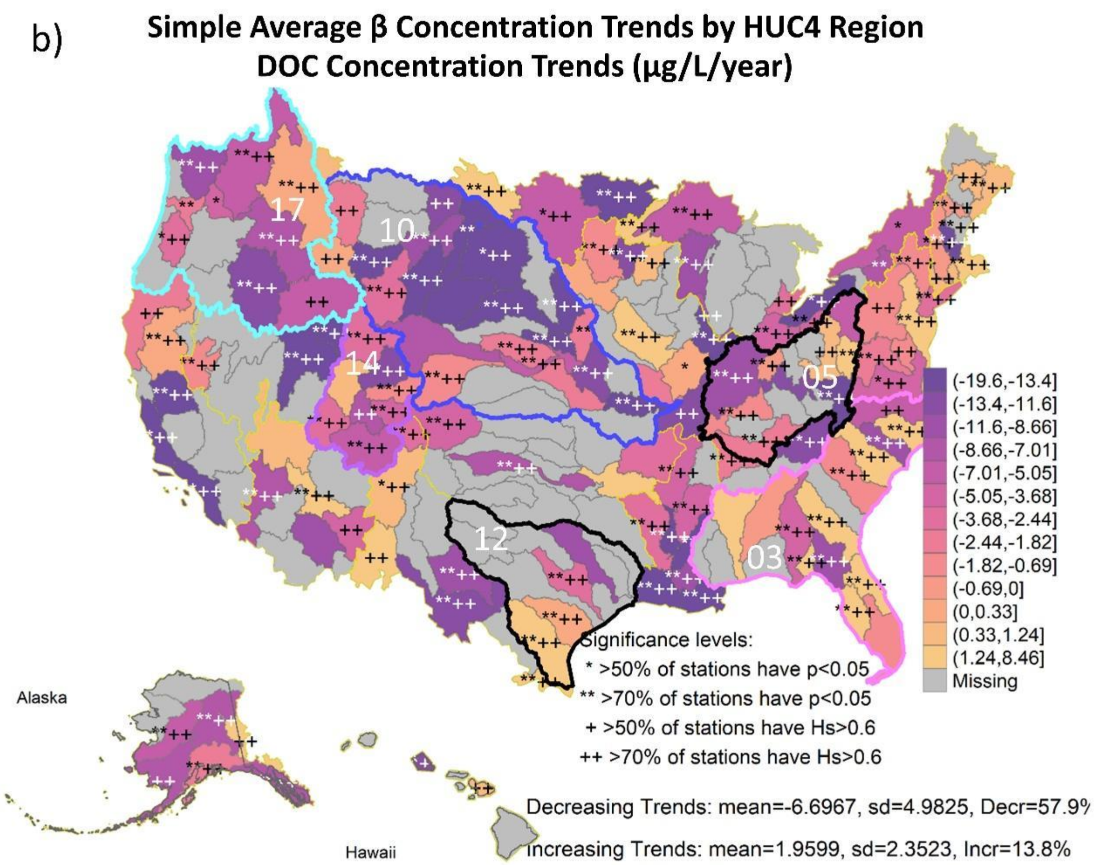
b)
Simple Average β Concentration Trends by HUC4 Region
DOC Concentration Trends (μg/L/year)
17
10
14
05
12
03
(-19.6,-13.4]
(-13.4,-11.6]
(-11.6,-8.66]
(-8.66,-7.01]
(-7.01,-5.05]
(-5.05,-3.68]
(-3.68,-2.44]
(-2.44,-1.82]
(-1.82,-0.69]
(-0.69,0]
(0,0.33]
(0.33,1.24]
(1.24,8.46]
Missing
Significance levels:
* >50% of stations have p<0.05
** >70% of stations have p<0.05
+ >50% of stations have Hs>0.6
++ >70% of stations have Hs>0.6
Alaska
Hawaii
Decreasing Trends: mean=-6.6967, sd=4.9825, Decr=57.9%
Increasing Trends: mean=1.9599, sd=2.3523, Incr=13.8%

525

Figure 4: Trends in a) DIN and b) DOC concentrations *C(t)* from 1970-2020 for the CONUS . Trends are shown from the average gap-filling method and β trends calculated for each station and aggregated up using Simple Averaging. Trends statistics are provided in Supplementary Table SB2 and SB3. Significance levels are indicated by the following symbols: * >50% of stations have $p<0.05$, **>70% of stations have $p<0.05$, + >50% of stations have $Hs>0.6$, and ++ > 70% of stations have $Hs>0.6$.

We highlight six HUC2 watersheds, four from Figure 3 (HUC2 #10, HUC2 #17, HUC2 #03, HUC2 #05) which represent the Groups a-d, and two additional HUC2 watersheds to contrast results (HUC2 #14 high-elevation, and HUC2 #12 low-elevation). Tables of DIN, DOC, and temperature statistics for these six watersheds are provided in Supplementary Table SB1, SB2, and SB3. Of these six basins, we find the largest DIN concentrations across the Texas Gulf Basin (HUC #12) (1.88 ± 3.04 mg/L), with average increasing rates of change ($\beta = 0.007 \pm 0.053$, $\beta_{MK} = 0.01 \pm 0.068$ mg/L/year). These rates contrast basins such as the Upper Colorado HUC #14, where 49.1% of stations show statistically significant declining trends ($\beta = -0.007 \pm 0.027$, $\beta_{MK} = -0.003 \pm 0.026$ mg/L/year). The Upper Colorado has the lowest concentrations of DIN among the six basins (0.33 ± 0.57 mg/L). In the Ohio Basin (HUC2# 05), average DIN concentrations are 1.78 ± 3.38 mg/L. The Ohio Basin shows the largest average rates of decline with a majority of stations (nSLP/nS >50%) showing statistically significant downward trends ($\beta = -0.03 \pm 0.14$ mg/L/year, $\beta_{MK} = -0.04 \pm 0.18$ mg/L/year). The number of stations showing significance of Mann-Kendall trend parameters generally agrees with the significance of the linear parameter (nSLP ≈ nSMKP). Trend statistical significance calculated with the Hurst Persistence parameter shows a larger fraction of stations have persistent trends than the linear or Man-Kendall parameters (see for example HUC#10, nSH = 251). Tables of statistics for all other HUC2 watersheds, statistical significance, linear, and Mann-Kendall trends are also provided in Supplementary Table SB1, SB2, and SB3.

We find the largest DOC concentrations across the South-Atlantic Gulf Basin (HUC #03) (13.36 ± 13.79 mg/L), with the lowest rates of DOC change ($\beta = 0.037 \pm 0.33$, $\beta_{MK} = 0.035 \pm 0.34$ mg/L/year). In the Missouri Basin HUC #10, average concentrations (5.78 ± 4.65 mg/L) are coupled with the largest rates of DOC concentration change ($\beta = -0.080 \pm 0.13$, $\beta_{MK} = -0.081 \pm 0.17$ mg/L/year). Tables of statistics for all other HUC2 watersheds, statistical significance, linear, and Mann-Kendall trends are also provided in Supplementary Table SB2. We also provide trend maps for all other water parameters in Supplementary Figure SB2-SB3.

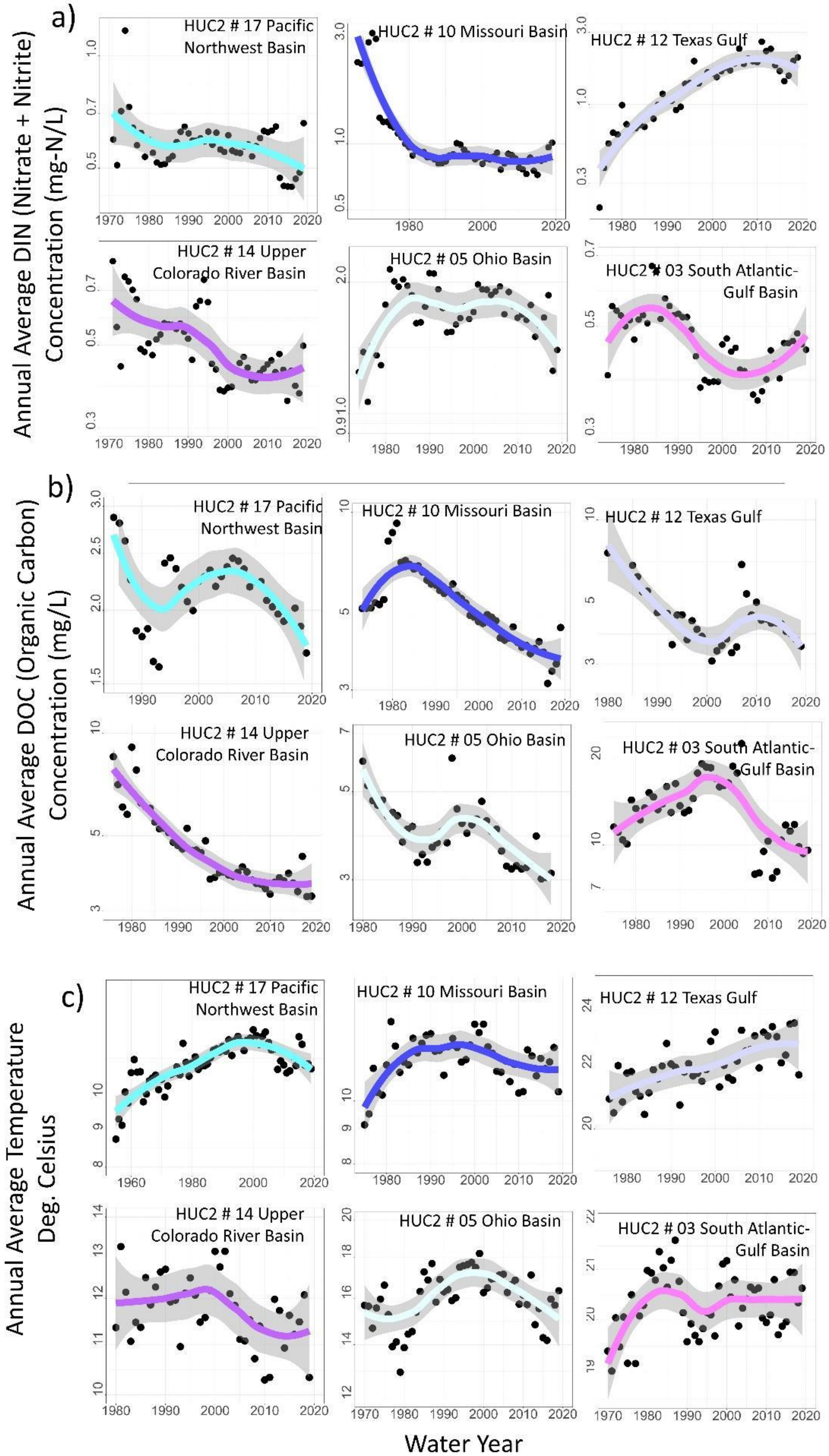
a)
b)
c)
Annual Average DIN (Nitrate + Nitrite) Concentration (mg-N/L)
Annual Average DOC (Organic Carbon) Concentration (mg/L)
Annual Average Temperature Deg. Celsius
HUC2 # 17 Pacific Northwest Basin
HUC2 # 10 Missouri Basin
HUC2 # 12 Texas Gulf
HUC2 # 14 Upper Colorado River Basin
HUC2 # 05 Ohio Basin
HUC2 # 03 South Atlantic-Gulf Basin
Water Year

559

Figure 5: Trends in DIN, DOC, and temperature from 1970-2020 for select HUC2 basins #17, 14, 12, 10, 05, and 03 are shown with the same colors corresponding to the groupings in Figure 3. Trends are shown from the average gap-filling method and β trends calculated for each station and aggregated up using Simple Averaging. Trends statistics are provided in Supplementary Tables SB1, SB2, and SB32.

3.3 The Role of Trends in Discharge on Trends in Exports across US Basins

Calculations of DIN exports (watershed losses) represent the combined effect of discharge and concentration in a basin (Equation 2) and are directly used in the calculation of watershed N-retention (Equation 4). Trends in DIN exports (linear β parameter for *Ex(t)* Mg/year) across all U.S. stations, aggregated to U.S. HUC4 watersheds show patterns of spatial variability in the direction (increasing or decreasing) and statistical significance similar to concentration trends (Figure 4, Supplementary Figure SB4). We found 34.8% of all stations (nS = 1136) across CONUS showed statistically significant decreasing trends in DIN exports ($\beta = -3.2 \pm 4.2$ Mg/year, outliers > 99th percentile and < 1st percentile removed) (Supplementary Figure SB4a). Another 22.3% of CONUS stations show statistically significant increasing DIN export trends ($\beta = 8.4 \pm 13.9$ Mg/year, outliers > 99th percentile and < 1st percentile removed). Aggregating all of the station export data *Ex(t)*) to all the HUC2 levels shows similar variability in magnitude and distribution of DIN export change across the CONUS (Supplementary Table SB4, Supplementary Figure SB5). Tables and maps of discharge, exports and their statistics are provided in Supplementary Figures SB6-SB9 and Tables SB5-SB7.

Trends in watershed exports are not only important for determining watershed retention metrics, but also for characterizing potential future N and C deliveries to coastlines given similar rates of change. The magnitude and direction of DIN export trends relative to the magnitude of yearly exports ranges between -16 to 24% per decade (all HUC2 decadal changes are provided in Supplementary Table SB4). Given a similar rate of change over the 2020-2030 decade, HUC #14, for example, would experience a decline in DIN exports of -16.9%, which is the largest declining rate relative to the other HUC2 basins, albeit quite low in magnitude (-66.9 Mg over the next decade). By comparison, HUC #17 would experience a decline in DIN exports of -4.6% over the next decade but a much larger magnitude (-127.7 Mg over the next decade). We aggregated these annual estimates of DIN and DOC trends to calculate total coastal exports from the land to the ocean from coastal abutting basins (specifically HUC2 #01, 02, 03, 08, 12, 13, 15, 17, 18, 19, 20). Across the coastal basins directly exporting N and C to the ocean, we found annual average coastal N and C exports are declining. Total dissolved inorganic nitrogen exports (sum of filtered nitrate, nitrite, ammonia, ammonium) have declined by approximately 60% over the past two decades (1970-2000: 9.4 Tg-N/year, 2000-2020: 3.72 Tg-N/year), and organic carbon exports have declined by approximately 80% over the past two decades (1970-2000:19.5 Tg-C/year, 2000-2020: 3.72 Tg-N/year).

While discharge is always the most significant contributor to yearly export magnitudes on an inter-annual basis, we found no conclusive evidence that decadal *trends* in discharge are the most significant contributor to decadal trends in exports (Figure 6). We found statistically significant discharge trends at < 10% of all CONUS stations (Supplementary Figure SB9, Table SB5). Correlations between trends in *Cn(t)* and *Ex(t)* were statistically significant at the $p<0.001$ level (Figure 6 a,b) while correlations between trends in *Qs(t)* and *Ex(t)* were statistically significant at the $p=0.04$ level (Figure 6 c,d). We observed that while changes (*trends*) in DIN and DOC exports are driven by *both* concentration and discharge (Supplementary Figure SB10, SB11), changes in exports were more often associated with changes in concentration rather than discharge (Supplementary Table SB8). When correlating decadal *trends* in discharge and concentration to *trends* in exports for all water parameters, we found directionally similar and statistically significant trends in *Cn(t)* and *Ex(t)* across more than 25% of stations. Conversely, we found directionally similar and statistically significant trends in *Qs(t)* and *Ex(t)* at <3% of stations (Supplementary Table SB8).

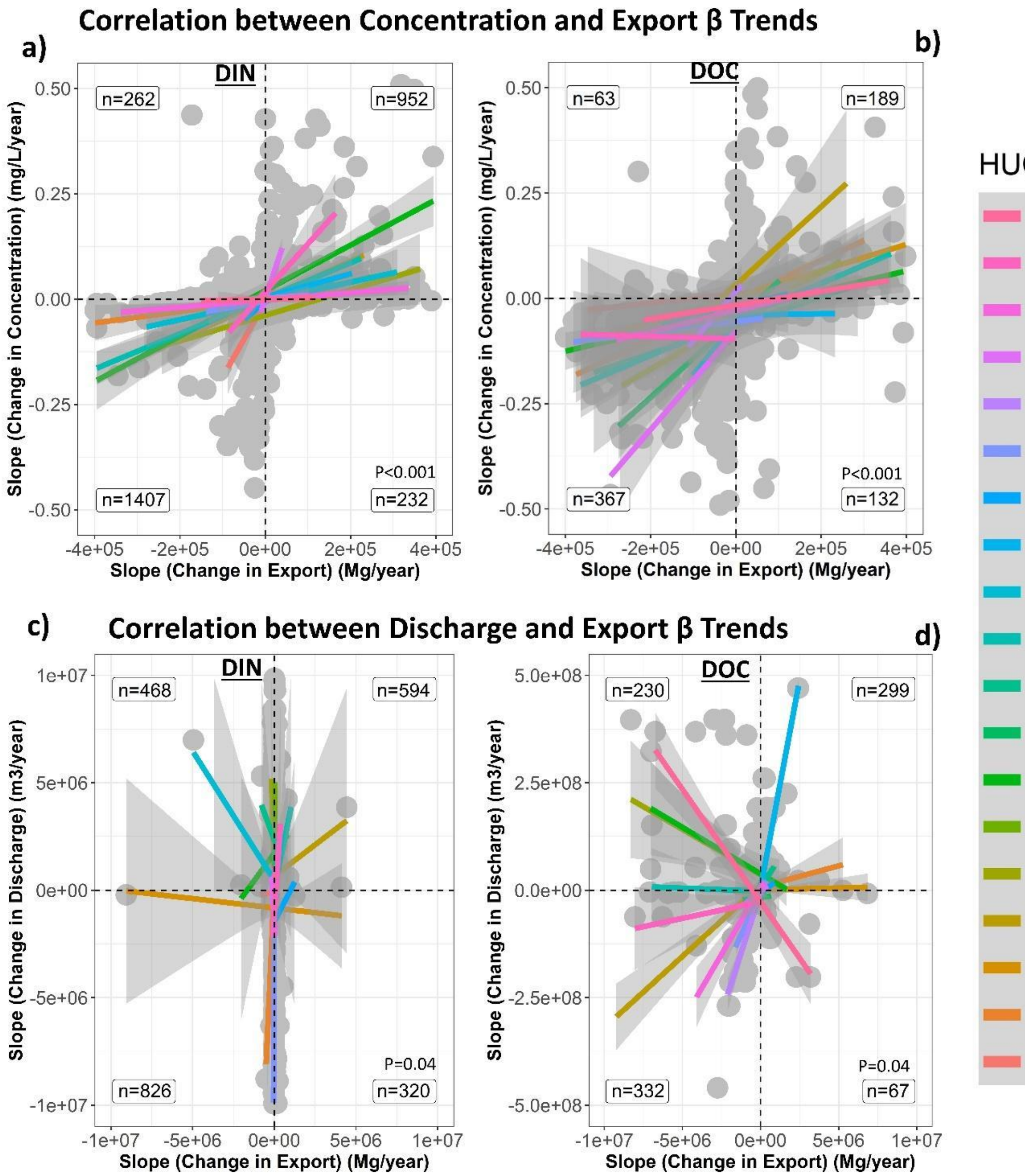

614

615 Figure 6: Correlations between trends in concentration and exports (a, b) and correlations
616 between trends in discharge and exports (c,d) for DIN and DOC. Each HUC2 basin correlation is
617 shown by the various colored lines. Within each quadrant, the number of data points (n) is
618 indicated. Total statistical significance for the aggregated trend correlation across all quadrants is
619 provided in each figure. Grey dots are individual stations that have both DIN and DOC trends.

When looking at correlations between trends in concentration and trends in export (a,b), most stations show similar directions of change (i.e. declining trends in concentration and declining trends in export) with statistical significance at the $p<0.001$ level. Correlations between trends in discharge and trends in export show dissimilar direction of change (i.e. increasing trends in discharge and decreasing trends in export).

3.4 Trends in Watershed Exports for NDVI-TDEP Groups

We examined trends in watershed exports to determine the degree to which watershed N-retention conditions and trends in DIN and DOC evenly divide across CONUS scale NDVI-TDEP groups conceptualized in our watershed hysteresis model (Figure 2). Trends in *E(t)* (Mg/year) for DIN and DOC obtained from all stations and aggregated by NDVI-TDEP groups from Figure 3 show distinct trends that support our conceptual model (Figure 7). DIN shows similar modes of variability across the TDEP-NDVI groups for both exports and yields: greater declines in exports (mean $\beta = -9.97 \pm 148.5$ Mg/year) and yields (mean $\beta = -0.001 \pm 0.04$ kg/hectare/year) in Group a, with steady increases across the TDEP-NDVI groups towards increasing exports (mean $\beta = 59.08 \pm 148.8$ Mg/year) and yields (mean $\beta = 0.13 \pm 0.56$ kg/hectare/year) in Group d. DIN export trends in Group a (declining trends) are associated with in-stream concentration declines (-0.0016 mg/L/year ±), and DIN export trends in Group d (increasing trends) are associated with in-stream DIN concentration increases (+0.0052 mg/L/year ±). DIN export trends show statistically significant differences between Groups a-d (Kruskall-Wallis test K.W. $p=0.0015$). DOC export trends are statistically significant between groups (K.W. $p=0.0117$) and show an interesting pattern of reversal from Group a to d: declines in exports are found for Group a and Group d (Group a mean β = -444 ± 574 Mg/year, Group d mean β = -854 ± 2253 Mg/year), but a greater proportion of increasing trends are found in Group b (mean β = 115 ± 114 Mg/year). DOC concentrations are declining for all groups except for Group c (0.0011 mg/L/year). Dissolved oxygen concentration trends are also statistically significant between TDEP-NDVI groups and show a general increase across groups A-D. Trends in *E(t)* (Mg/year) and *Y(t)* (kg/hectare/year) by NDVI-TDEP group for all water parameters are provided in Supplementary Figure SB12. Seasonally aggregated barplots are provided in Supplementary Figure SB13.

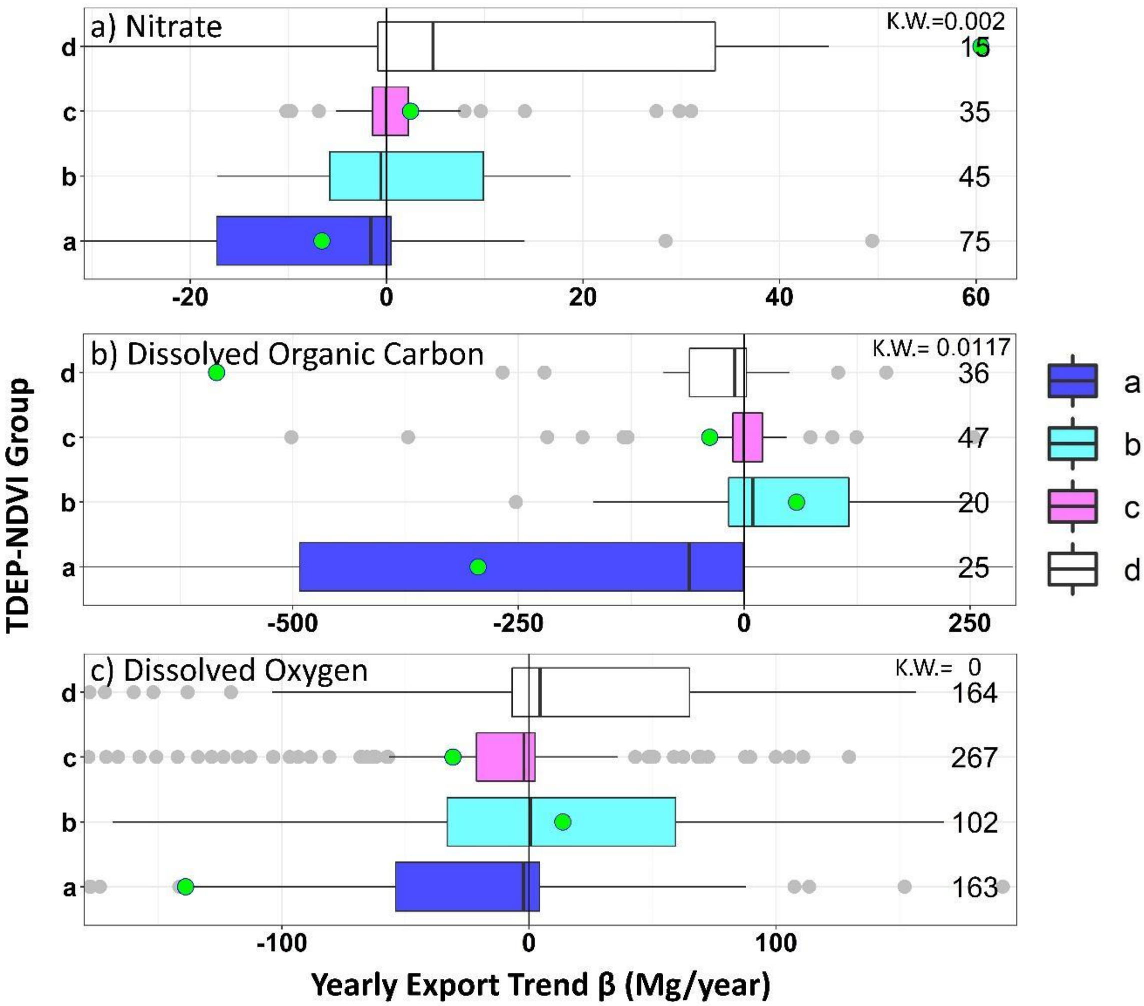

Figure 7: Box plots of the export and yield data separated by river chemical parameters separated and colored by NDVI-TDEP groups. Boxplots show the median as the middle line, upper (75%) and lower (25%) quartiles as ends of the box, and upper and lower fences representing 1.5 times the inter-quartile range. If there are outliers more or less than 1.5 times the upper or lower quartiles, respectively, they are shown with grey dots. All trend results are colored based on the associated NDVI-TDEP group. The number of statistically significant stations (nS), the mean and standard deviation are shown next to each box. All statistics were calculated using only

stations with statistically significant trends ($p<0.05$). As a reminder of the TDEP-NDVI grouping representations, Groups a (+TDEP, +NDVI), Group b (+TDEP, -NDVI), Group c (-TDEP, +NDVI), and Group d (-TDEP, -NDVI).

3.5 Retention across U.S. Basins

Trends in watershed retention (slope of Equation 1 and 4, TDEP inputs minus watershed exports) across all U.S. HUC4 basins reveals wide variability in retention patterns (Figure 8) when compared by region or NDVI-TDEP group. The lowest retention values across the CONUS occurs in the Midwest region (HUC2 #07 mean retention = 35%) (Figure 8 a, Supplementary Table SB9) and corresponds with the largest declining N-retention trends. By contrast, most regions across the U.S. have high watershed N-retention (>90%) and sustain high retention values over time from slopes closer to zero. Retention calculations across CONUS also reveal differences when assessed between NDVI-TDEP groups (Figure 8b). Most HUC8 watersheds classified as Group a, retain close to 100% of incoming atmospheric TDEP (median = 98.6%, mean = 93.3%, s.d. = 17.6%) (Figure 8b). Watersheds classified within Group d retain about one-half to two-thirds of incoming TDEP (median = 77.8%, mean = 61.8%, s.d. = 42.1%). As expected based on the proposed conceptual model (Figure 2), once watersheds become N-saturated (occurs around Group b), retention of incoming N-deposition decreases and more is lost directly to watershed exports leading to lower retention values (Groups c and d). Watershed N-retention was also found to decline with increasing in-stream nitrate concentrations reflecting the potential saturation of biogeochemical processes with increasing concentrations (Supplementary Figure SB14). Retention statistics and plots calculated for each HUC2 basin are provided in Supplementary Table SB9 and trends for the selected HUC2 basins are shown in Supplementary Figure SB15.

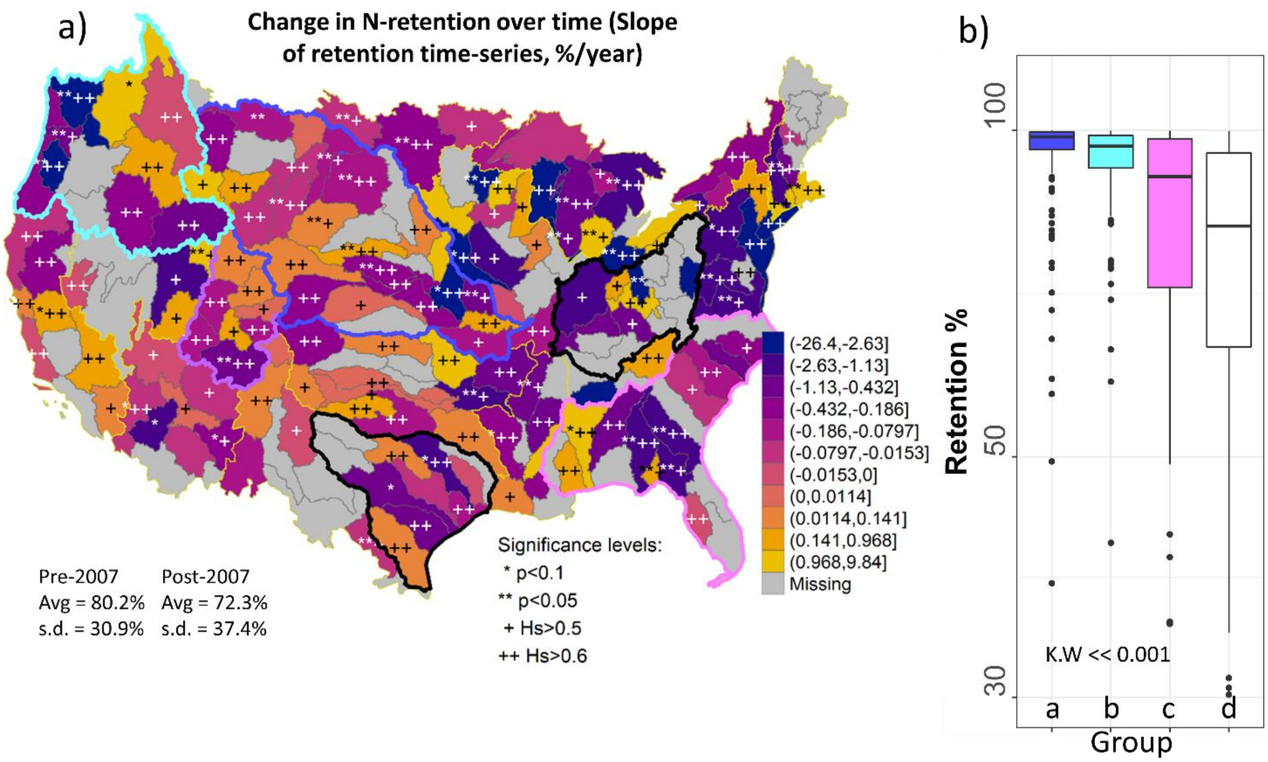

Figure 8: a) Spatial distributions of N-retention trends (% Retention change per year) for N are shown for HUC4 watersheds across the CONUS. b) Box plots of N retention are shown for the different TDEP-NDVI groups and show statistically significant differences (K.W. << 0.001). As a reminder of the TDEP-NDVI grouping representations, Groups a (+TDEP, +NDVI), Group b (+TDEP, -NDVI), Group c (-TDEP, +NDVI), and Group d (-TDEP, -NDVI).

Across HUC8 watersheds, retention is found to vary as a function of land-use characteristics and NDVI-TDEP groups (Figure 9). Retention varies across the different NDVI-TDEP groups in a similar fashion to that shown in Figure 8b with larger retention values on average in Group a (92.5% ± 19.5 %) and lower retention values in Group d (61.1% ± 40.6 %). For each land-cover class, K.W values for differences between NDVI-TDEP groupings are statistically significant. Forest land cover shows highly variable retention across the NDVI-TDEP groups with the lowest retention found in Group b (-13.0% ± 36.9 %). The negative value for Group b indicates an additional source of N is present (outputs > atmospheric inputs). Planted land-cover types, which include cultivated crops and pasture/hay, also show a general decline in retention from Group a (91.9% ± 20.5%) to Group d (51.5% ± 43.5%), but with much larger distribution of values in Group b. Wetland land cover types show close to 100% retention for NDVI-TDEP Groups a and b, and then trend downward for Groups c and d. Maximum land-cover types and changes by HUC2 basin are provided in the Supplementary Figure SB16. Maximum land-cover types and changes by NDVI-TDEP group and year are provided in the Supplementary Figure SB17.

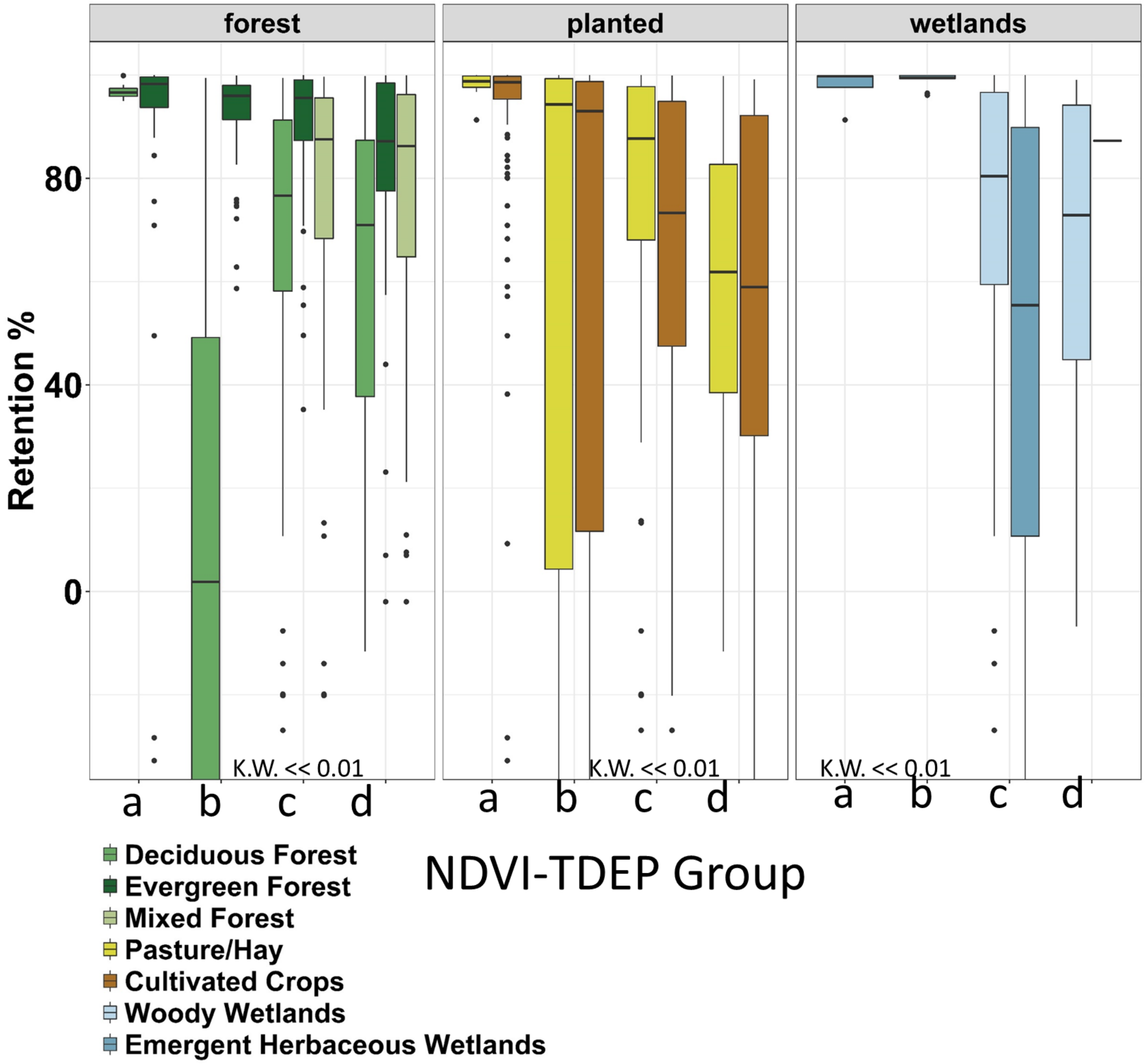

Figure 9: N-retention across NDVI-TDEP groups (assessed at the HUC8 level) are further refined by different land cover class and types (forest, planted, and wetlands). Colors represent the different land-cover groups within each broad land-cover class. Within each land cover class category, box plots of N-retention distributions are provided across the NDVI-TDEP groups and the K.W. test of statistical significance is shown.

Comparing the total percent of variance in watershed N-retention explained by the four groups of interest (land cover, NDVI-TDEP group, Elevation, and stream factors which include stream temperature/DOC concentrations), our results indicate that land cover may not be the primary controlling factor on watershed N-retention (Table 2). The total percent of variance in watershed N-retention explained by land cover type ranges between 0.15-30.8 % (average 9.97%) which is the third largest factor among the four explanatory groups. NDVI-TDEP groups primarily explain, on average, a greater percent of the variance in watershed N-retention (range 4.03-45.14%, average 16.13%). Stream factors which include the combined temperature and DOC concentration dataset explain the second largest percent of variance in watershed N-retention (range 0.04-36.85%, average 13.23%). Regionally, land cover is a second order control within the Lower Mississippi River basin (HUC #08, explains 30.8% of variability in N-retention) despite land cover being of lesser importance in the five other HUC2 basins that contribute directly to the Lower Mississippi (Arkansas White Red HUC2 #11, Missouri HUC2 #10, Upper Mississippi HUC2 #07, Ohio HUC2 #05, Tennessee HUC2 #06). The Mid-Atlantic Basin (HUC2 #02) is the only basin where land cover is identified as a primary co-variate to watershed N-retention. The inclusion of the land-cover change dataset explained such a significantly low percentage of variability (<0.0001%) that we do not show those results here and we excluded that variable from the analysis.

Table 2: Percent of variability in watershed N-retention explained by the four different variables of interest for each HUC2 basin. The percent of variability explained by each variable was calculated using the ANOVA statistical analysis and statistical significance of each variable is

indicated in parentheses. The percent of the retention variance attributable to each explanatory variable is shown based on calculations at the HUC8 scale within each HUC2. The blue cells indicate the variable with the maximum explained variance among the four groups shown for that particular HUC2.

Percent of Variability In Watershed N-Retention Explained

HUC2	Maximum Land Cover Class	NDVI-TDEP Group	Elevation	Stream Factors (Temperature and DOC)
01	0.25(0.144)	11.69(0)	0.5(0.038)	19.82(0)
02	20.16(0)	6.51(0)	0.28(0.012)	11.49(0)
03	2.98(0)	15.91(0)	0.07(0.372)	6.88(0)
04	7.45(0)	12.52(0)	0.68(0.001)	11.39(0)
05	9.95(0)	12.27(0)	1.1(0.025)	11.19(0)
06	3.48(0.008)	17.12(0)	4.52(0.003)	13.12(0)
07	19.29(0)	34.83(0)	0.09(0.14)	5.47(0)
08	30.8(0)	45.14(0)	0(0.862)	12.53(0)
09	8.08(0)	35.4(0)	5.79(0)	6.08(0)
10	9.19(0)	11.09(0)	4.03(0)	6.89(0)
11	11.94(0)	16.95(0)	0.82(0)	3.55(0)
12	14.57(0)	4.03(0)	0.21(0.095)	21.73(0)
13	0.16(0.398)	4.77(0)	2.11(0.002)	12.78(0)
14	10.07(0)	6.74(0)	1.6(0)	32.64(0)
15	5.92(0)	17.56(0)	29.39(0)	4.57(0)
16	1.72(0.002)	19.13(0)	1.61(0.003)	24.89(0)
17	0.87(0)	16.8(0)	0.45(0)	36.88(0)
18	22.75(0)	6.91(0)	0.98(0)	31.74(0)
Average	9.97%	16.40%	3.01%	15.17%
	1	9	1	7

* p-values are shown in parentheses

3.6 Modalities of Watershed Retention and Hysteresis

TDEP and NDVI are important controlling factors on watershed N-retention patterns, and our results demonstrate evidence for watershed N-hysteresis across the range of deposition environments (Figure 10a). Watersheds with high retention capacity (where >90% of N is retained, red dots) show a trend toward increasing NDVI with TDEP—watersheds with high retention capacity have the potential to store excess N in biomass and likely become N-saturated as TDEP increases (TDEP range 3-10 kg/hectare/year, NDVI range 0.2-0.6, Figure 10a). Watersheds with low retention capacity (<20% of N is retained, blue dots) are N-saturated or undergoing recovery from N-saturation and show a different relationship with NDVI and TDEP than the high-retention capacity group (Figure 10a). Low-retention watersheds undergoing reversal from N-saturation show that NDVI remains high for all values of TDEP and appears to decline quite significantly once TDEP is < 3 kg/hectare/year. Our results show that the relationship between NDVI and TDEP differs depending on how saturated the watershed is and the state of NDVI and TDEP. Lower initial values of NDVI are associated with the increasing NDVI group while larger initial values of NDVI are associated with the decreasing NDVI groups (Figure 10c). Similarly with TDEP, lower values are within the increasing TDEP category, and larger values are in the decreasing TDEP category (Figure 10b). Watersheds with a high N-retention capacity are generally associated with regions of increasing TDEP and NDVI patterns, while watersheds with a low N-retention capacity are generally associated with regions of decreasing NDVI and TDEP patterns. As the first line of evidence supporting N-hysteresis in watersheds, these generalizable patterns suggest that eventual recovery from excess N-deposition may include a lagged response and a legacy of compromised forest health.

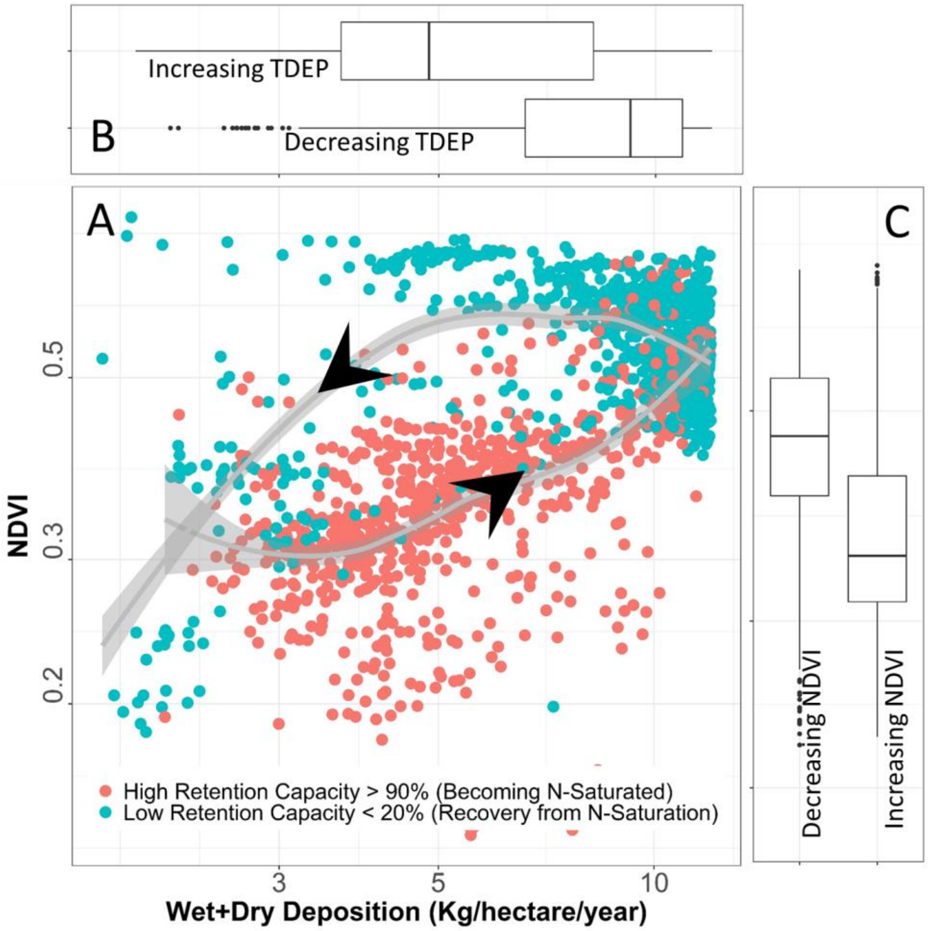

772

773 Figure 10: Watershed N Retention capacity follows a hysteretic loop across the different stages
774 of TDEP and NDVI. a) Scatterplot of NDVI and TDEP values at the HUC8 scale colored by
775 high (red dots) and low (blue dots) watershed N-retention capacity for all water years that are
776 available. High retention capacity HUC8 watersheds are those that retain most atmospheric
777 deposition and have very low losses in stream exports leading to retention that is >90% (Group a,
778 Figure 2). Low retention capacity HUC8 watersheds are those that lose most atmospheric
779 deposition to stream losses leading to retention that is < 20% (Group d, Figure 2). B) Boxplot
780 distribution TDEP values (associated with x-axis) grouped by trends in TDEP. C) Boxplot
781 distribution of NDVI values (associated with y-axis) grouped by trends in NDVI. Since higher N
782 retention watersheds are still experiencing increases in TDEP and increases in NDVI (red dots,

Group a from Figure 8b), a positive relationship is identified between TDEP and NDVI as these watersheds become N-saturated over time. In lower N retention watersheds (blue dots, Group d from Figure 8b), or more specifically those that are recovering from N saturated conditions, there is a hysteretic loop such that declines in TDEP are followed by declines in NDVI but follow a very different response pathway than watersheds with increasing TDEP patterns. The lines and grey area surrounding the lines is a “loess” regression to the high retention group and a separate regression to the low retention group. The confidence interval shown is the 95% confidence intervals around the mean of the predictions. Loess (local regression) is a non-parametric approach that fits multiple regressions in local neighborhood.

Hysteresis and one-way transition patterns of watershed N-retention and loss for a few select individual HUC8 watersheds reveal varying modalities of N-retention and recovery (Figure 11). The highlighted watersheds with permanent changes (i.e. one-way transition to a new steady-state) are represented by maximum land cover types of Evergreen Forest-72.34% (permanent increase in retention, Figure 11a), and Deciduous Forest-38.08% (permanent decrease in retention, Supplementary Figure SB18). A decline in Evergreen Forest is also observed (86.16% coverage in 2001 to 72.34% in 2016) and associated with a one-way increase in retention and decreases in losses (Figure 11a). One-way declines in retention and increases in losses are found in HUC8 #02080103 (Rapidan-Upper Rappahannock, Virginia) with a dominant land cover type classified as Deciduous Forest (Supplementary Figure SB18). The percent of the dominant land cover class (Deciduous Forest) does not change much over the 2000-2016 time period, however, some land cover change is evident (e.g., a 1.1% loss of Pasture and conversion to Cultivated Crops, and Grassland) (Figure 11d). The watersheds with one-way increase and loss patterns (Figure 11a, and Supplementary Figure SB18) are notable because they potentially represent watersheds that have transitioned beyond an equilibrium state in response to N deposition or other changes.

Clockwise and counterclockwise hysteresis patterns representing a system's reversion back to initial conditions also emerge (Figures 11b, d, Supplementary Figure SB19). In some cases, the watershed moves to a new shifted state represented by changes in both retention and loss, or the watershed returns to the original state represented by values of retention and loss that are at or near the initial state (Figure 11b,d). This might be interpreted as having an unperturbed biogeochemical cycling capacity such that it can sustain significant deviations from the original state and still return to the original state. Watersheds with Retention ≈ 0% are rare (n=14 out of 2119 HUC8 watersheds) and represent watersheds with close to equal inputs (TDEP) and outputs (losses or Yields), 3 of which occur in the Upper Mississippi (HUC2 #07). These watersheds may have a significantly perturbed N-cycle due to point-scale wastewater and agricultural inputs, and only represent a steady state condition wherein inputs are equivalent to outputs. However, they could also potentially represent a subset of watersheds lacking significant biogeochemical capacity. Watersheds with outputs greater than inputs (greatly perturbed) are similarly rare, representing <5% of watersheds (n=103 out of 2119 HUC8 watersheds), 29 of which are in the Upper Mississippi (HUC2 #07). Watersheds representing near pristine conditions, with retention close to 100%, represent ~12% of HUC8 watersheds (n=251 out of 2119 HUC8 watersheds), 65 of which are in the Missouri Basin (HUC2 #10, 58% Grassland/Herbaceous, Supplementary Figure SB16). The perturbed, greatly perturbed, and pristine HUC8 watersheds are listed in Supplementary Table SB10 and included as text files with the data package associated with this manuscript. While we highlight individual watersheds here, we also recognize many watersheds do not have clear patterns and require much greater interrogation into underlying processes.

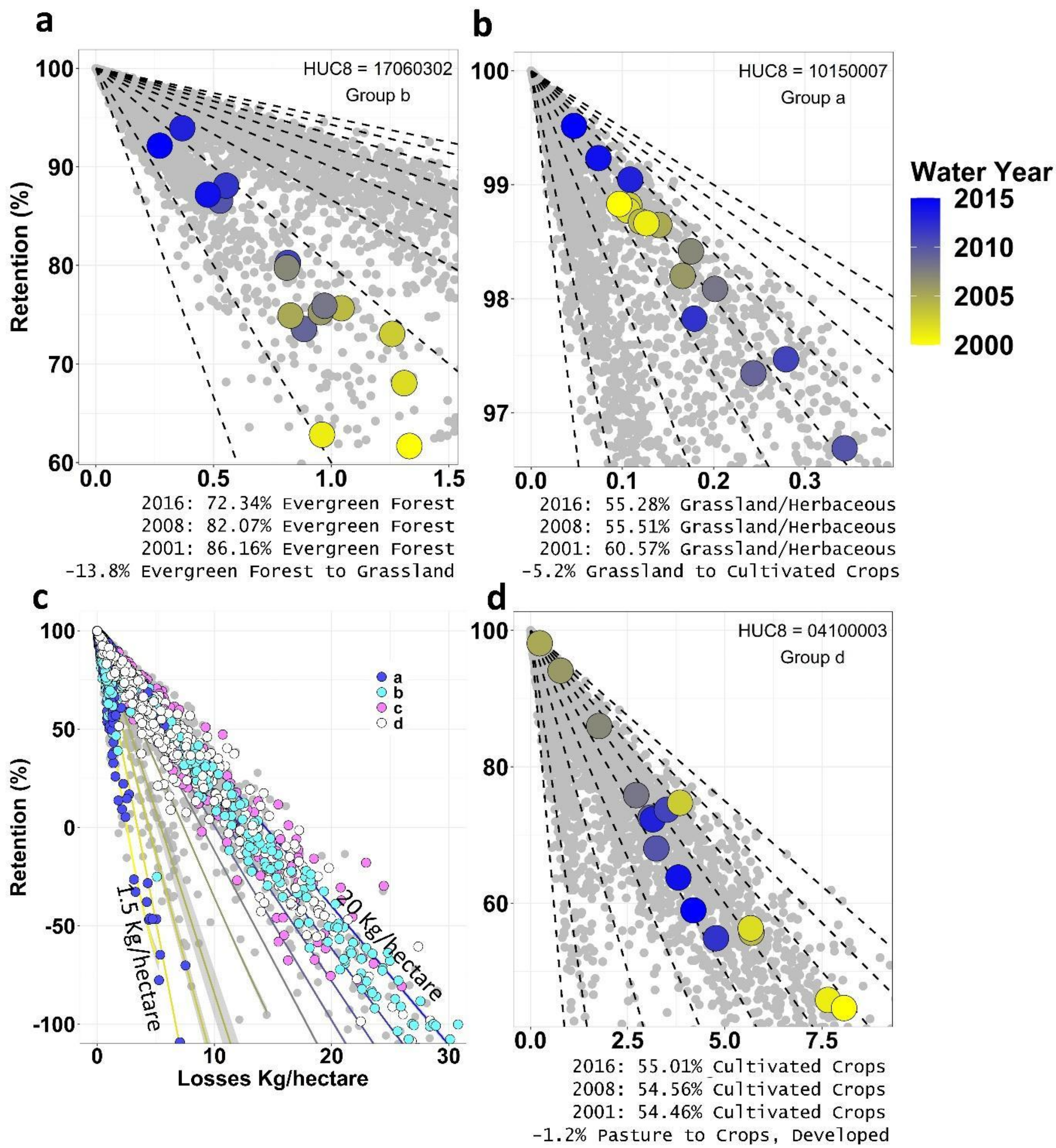

Figure 11: Scatter plots and hysteresis curves of HUC8 watershed N-retention (%) (y-axis) and loss (x-axis) (kg/hectare) in individual HUC8 watersheds. Grey dots in each figure represent the

scatter of N-retention and losses from all HUC8 watersheds within the particular HUC2 of focus (i.e. HUC8 #04100003 is in HUC2 #04). Dashed lines represent lines of equal TDEP (kg/hectare) ranging from 1.5-20 kg/hectare also shown by solid lines in c. The colored dots represent the yearly retention and loss for the individual HUC8 specified. Colors represent the water year and are increasing from the year 2000 (yellow) to 2015 (blue). One-way transition and hysteresis patterns are visible within these examples. Percentages below each figure represent the land cover type with the maximum percentage coverage for each year and the largest land-cover change category. a) A one-way transition pattern to a new steady-state is observed in HUC8 #17060302 which falls within retention group b, b) A hysteresis pattern is observed in HUC8 #10150007 which falls within retention group a. Retention declines then returns to the initial condition. c) Retention and loss patterns for all HUC8 watersheds colored by NDVI-TDEP group, d) A hysteresis pattern is observed in HUC8 #04100003 which falls within retention group d. Retention increases then returns to the initial condition.

4.0 Discussion

In this study, we examine the degree to which CONUS scale atmospheric deposition patterns, vegetation trends, and stream trends can be potential indicators of watershed N-saturation, retention, and recovery conditions, and how watershed N retention and losses vary over space and time. We provide evidence for the hysteresis behavior of N-saturation and retention in watersheds using a time series of CONUS stream losses relative to CONUS atmospheric deposition inputs and NDVI. We highlight watershed N-retention patterns across groups of atmospheric deposition and vegetation productivity/biomass to advance understanding of stream trends as indicators of watershed N conditions, and reveal patterns of watershed N-hysteresis (recovery) or transition patterns.

4.1 Stream Trends Reveal Watershed N-Hysteresis Patterns

Several lines of evidence here support the hysteretic conceptual model of watershed N retention and recovery (Figure 2). First, we found that atmospheric deposition (TDEP) and vegetation (NDVI) groups that display combinations of strong positive or negative trends over time, are associated with patterns of stream exports that uniquely indicate the stage of watershed N-saturation (Figure 8) and reveal modalities of watershed N-retention hysteresis or one-way transition patterns (Figure 11). As a reminder of the TDEP-NDVI grouping representations, Groups a (+TDEP, +NDVI), Group b (+TDEP, -NDVI), Group c (-TDEP, +NDVI), and Group d (-TDEP, -NDVI). In particular, we found regions with increasing TDEP and increasing NDVI *trends* (Group a, Figure 2) have close to 100% N-retention (Figure 9c), become increasingly N-saturated over time (Figure 11), and are associated with the strongest declines in DIN and DOC exports (Figure 8). Conversely, we find a tendency towards increasing trends in DIN exports and much lower retention in regions associated with TDEP-NDVI Group d where watersheds retain about 50 - 66 % of incoming TDEP. Second, trends in DIN export that coincide with trends in DOC export also help to identify the stage of watershed N-retention and direction of change based on our updated N-hysteresis conceptual model. Since DOC movement to streams is a function of the size of the watershed C pool, in-stream DOC concentration measurements combined with DIN measurements can provide an important proxy of catchment responses to N deposition and input. Third, by examining how watershed N-retention has changed over time, we found that watersheds display a variety of types of recovery (hysteresis) or non-recovery (one-way) patterns. Our findings agree with the hypotheses presented by Lovett et al. (2018) that areas at late successional stages (i.e., those in Group d) should show much less retention than their aggrading counterparts (Group a). Our retention estimates are within the published range of values for watersheds (Boyer et al., 2002). This work can provide value to future interpretation of in-stream trends and provides a new conceptual model such that in-stream DIN and DOC *trend* signatures can be used as *indicators* of aggregated watershed N-retention status (Gilliam et al., 2019; Goodale et al., 2003, 2005).

4.2 Drivers of N-retention, and hysteresis patterns across the CONUS

We found that regional trends in stream exports were more often correlated to trends in concentration rather than trends in discharge. This reveals that the dominant contributing factor to *changes in N magnitude and the trend trajectory* of exports are more often determined by changes in concentrations, rather than flows. This emphasizes the significant role of 1) watershed biogeochemical cycling and processes (soil and biomass immobilization, in-stream biogeochemistry etc.) across the critical zone as major factors shaping in-stream concentrations, and 2) the significant role of environmental physical/chemical conditions (TDEP-NDVI group) that facilitate uptake and retention of N. While the lack of influence of discharge has been noted previously (Goodale et al., 2003; Lucas et al., 2016), drivers of trend trajectory in exports can be hydrological, biogeochemical, or an external factor (e.g. agriculture), whereas, the observed trends in discharge and concentrations can be indicators of changing watershed N functionality through vegetative, soil, or in-stream biogeochemical pathways (Arora et al., 2020). For example, the insignificant role of discharge trends on determining overall trends in exports and concentrations may be more directly related to the stage of watershed N-saturation, evapotranspiration control on depth of hydrological flow paths, and newly acquired access of flowpaths to stores of older N and C not readily assessable prior to transitions in TDEP-NDVI stage (Barnes et al., 2018). Indeed, residence times of water versus N particles within a watershed are different and can vary from years to decades (Sinha & Michalak, 2016). Recent work in watershed acid-rain mitigation experiments suggests that the ‘flashiness’ of N export during storm events might be an important indicator of watershed N-retention and saturation status because of shifts in N sourcing from more distal and shallow parts of the watershed (Marinos et al., 2018). Despite the lack of significant trends in discharge observed in our study, more work will be needed assessing how hydrological conditions coincide with broad scale physical/chemical conditions as described by TDEP-NDVI patterns that impact flow paths and access to different stores and cycling of C and N in landscapes.

4.3 In-stream processes

The second-largest factor explaining variability in watershed N-retention across HUC2 basins was in-stream temperature and DOC concentration trends (Table 2). This result provides evidence that in-stream measurements can potentially be *indicators* of watershed functionality by interpreting stream signals as aggregated measurements and proxies, namely *integrators*, to those upstream watershed biogeochemical conditions. The consequence of changing N and C transfer from the terrestrial to the aquatic setting is the mediation of in-stream assimilation and hyporheic redox conditions at downstream locations. In-stream and hyporheic biogeochemistry provides an important control on stream exports once nutrients reach the stream through in-stream assimilation and hyporheic denitrification (Arora et al., 2016; Cejudo et al., 2018; Hood et al., 2017). Declining stream N exports due to increased watershed N retention may lead to steady or increasing DO concentrations in downstream ecosystems and transition to oligotrophic conditions (Craine et al., 2018; Groffman et al., 2018). Changes in aquatic primary production can occur in response to changing nitrogen inputs (from atmospheric deposition and watershed delivery) and seasonality (Bernhardt & Likens, 2004), which can shift denitrification rates and patterns through direct and indirect coupling to labile carbon exudates and oxygen conditions (Heffernan & Cohen, 2010). Conversely, in low-elevation or more anthropogenically impacted sites, rising temperatures and increases in N transfer to streams could coincide with declining DO concentrations and more eutrophic conditions, greater in-stream N-assimilation, particularly in N-limited water bodies (Beaulieu et al., 2011; Bernhardt et al., 2002; Halliday et al., 2013), and greater hyporheic denitrification (Bernhardt et al., 2005; Duncan et al., 2013, 2015; Maavara et al., 2019; Mulholland et al., 2009; Newcomer et al., 2018; Seitzinger et al., 2006). We found that watershed N-retention efficiency declines with increasing nitrate concentrations suggesting that biogeochemical cycles can saturate as well, which is in line with studies reporting declines in denitrification efficiency with increasing concentrations (Mulholland et al., 2009) (Supplementary Figure SB14). The influence of stream factors on watershed N-retention before land use/cover was a surprising aspect of this analysis. Because stream and hyporheic residence times are so short, this conclusion indicates that instream processes are probably substantially more influential than expected, in terms of the overall magnitude of control on stream exports.

4.4 Confounding factors

We found that watershed retention is high (>70% for most watersheds across the U.S.) relative to atmospheric inputs, a finding similar to other published work (Lovett et al., 2000). It is important to note that any external contributions to in-stream DIN concentrations and exports not accounted for in this study (i.e. agriculture) would be additional input terms in the retention equation. These retention estimates are likely an underestimate of watershed N retention because there is uncertainty related to source terms from the lack of information on anthropogenic inputs across these watersheds. We do not account for agriculture or wastewater inputs to our retention equation, which means that our retention estimates are potentially significant *underestimates* of retention. Since exports and TDEP are the measured values in the retention equation, we estimate that in the most intensively managed agricultural regions, we are underestimating retention by 50-100% (25 kg/hectare/year)(Van Meter et al., 2016).

Wastewater and agricultural inputs were not a direct focus of our study, although their impacts on N and C loading and concentrations are estimated to be large at point scales especially in urban settings (Rice & Westerhoff, 2017; Stets et al., 2020). We found that in urban areas, across all TDEP-NDVI end-members, retention was consistently lower than in the other land cover groups (Supplementary Figure SB19). This is driven by larger exports relative to deposition indicating the potential for these internal point sources. Additionally, TDEP-NDVI end-member Group d experienced the largest change in urban land cover relative to Group a-c (average change of 12.1% in watersheds within Group d) over this time period (Supplementary Figure SB17). Group d regions were found to be low-retention watersheds with declining NDVI and declining TDEP, and found in lower-elevation regions which is often where new urban developments are occurring. Conversely, Group a regions were more likely to be found in higher elevation settings (Supplementary Figure SB20). Thus there is some co-variability between NDVI-TDEP groups and elevation such that decreased N exports in low-elevation regions can potentially be explained by a greater number of management practices in low-elevation waters.

While we acknowledge that water regulation from the 1972 Clean Water Act could be the main reason for declining DOC and DIN with these low-elevation watersheds, and lower overall N-retention (Stets et al., 2020), the role of in-stream, hyporheic, and landscape processes has consistently been shown to be effective mediators of stream N even at low to moderate land use intensity (Mulholland et al., 2008). Because direct anthropogenic loadings (wastewater, agriculture) circumvent a significant portion of the landscape biogeochemical cycles, declines in N and C from anthropogenic controls mask the importance of streams as critical bioreactors. The magnitude of this landscape and stream bioreactor is visualized within Table 3. In watersheds where both deposition and exports are measured and are of the magnitude 5 kg hectare^{-1} and 1 kg hectare^{-1} respectively (over 964 HUC8 watersheds have deposition >5 kg hectare^{-1} and exports <1 kg hectare^{-1}), if we assume agricultural and wastewater inputs are large (18 kg hectare^{-1}), this indicates that the magnitude of the watershed stream-landscape bioreactor grows increasingly with the scale of additional input (Table 3). This underscores the importance of the watershed bioreactor as a significant control on in-stream N and C (Mulholland et al., 2008).

Table 3: An example watershed showing how retention and the bioreactor capacity of the watershed changes with increasing agricultural inputs.

Deposition	Agricultural and Wastewater Inputs	Exports	Retention	Magnitude of the watershed bioreactor
Kg hectare^{-1}	Kg hectare^{-1}	Kg hectare^{-1}	%	Kg hectare^{-1}
5	0	1	80.0%	4
5	2	1	85.7%	6
5	4	1	88.9%	8
5	6	1	90.9%	10
5	8	1	92.3%	12
5	10	1	93.3%	14
5	12	1	94.1%	16
5	14	1	94.7%	18
5	16	1	95.2%	20
5	18	1	95.7%	22

Surprisingly, while we found that land cover and, in particular, land cover change data was the least significant factor controlling N export and retention, we acknowledge that consideration of potential drivers of some stream N trends depends somewhat on to what extent these watersheds receive urban, wastewater, or agricultural N inputs and how these have changed. For example, we found more spatially consistent decreasing trends in stream dissolved ammonia and ammonium exports and concentrations across the CONUS that might be more likely to reflect change in fertilizer or sewage N inputs (Supplementary Figure SB7). The lack of significance between watershed N-retention and land cover/change data may also point to legacy N in watersheds. Given the history of N deposition and anthropogenic application on ecosystems, there is great potential for lagged responses and geochemical stationarity in stream N and C because of significant water and N residence times (Basu et al., 2010).

Other confounding factors not included in this analysis are the occurrence of extreme event hydrological conditions (Argerich et al., 2013), shifts in the abundance of dominant vegetation within classes (Argerich et al., 2013; Bernal et al., 2012; Compton et al., 2003; Rhoades et al., 2017; Sudduth et al., 2013; Van Breemen et al., 2002), changes in vegetation aboveground biomass and plant populations in response to varying alpine snow-hydrological conditions (Hubbard et al., 2018), riparian controls (Rogers et al., 2021), and changes in reforested areas that could explain an overall decline in NO_3^- export within the stream (Bernal et al., 2012). In other studies, declines of in-stream N have been found in regions with greatest soil N accumulation and during the growing season indicating a biologically mediated trend in DIN and no correlation with hydrology (Lucas et al., 2016). Similar to Goodale et al., (2005) we find patterns in DOC concentrations across these watersheds that support the hypothesized mechanism that enhanced ecosystem productivity increases fluxes of labile carbon from the soil to the stream, enhancing denitrification leading to declining stream N trends. Finally, the importance of climatic controls on soil N processes cannot be emphasized enough. Longer growing seasons, with warmer climates and elevated CO_2 have been shown to change nitrogen and carbon availability in terrestrial soils (Terrer et al., 2018). Plant uptake and N mineralization both respond to soil moisture, temperature, and climatic patterns such that any changes in the rate or timing of these processes can tilt watersheds beyond their ability to retain or release nitrogen in a hysteretic manner, and their ability to function as a significant bioreactor.

5.0 Conclusion

In many watersheds across the CONUS, stream exports of DIN have been declining and show enduring legacies from N-deposition and acid rain. To examine large scale controls on stream DIN and DOC concentration and export trends, we developed an updated hysteresis conceptual model of watershed N-retention and examined how two main controlling landscape-scale factors (TDEP and NDVI) can be used to group watersheds by patterns of stream loss and watershed retention. Our hysteresis conceptual model provides a novel framework for which to assess watershed N-retention and recovery patterns as indicated by stream DIN and DOC trends. Our conceptual model is validated with a quantitative analysis of stream data (DIN, DOC, temperature), NDVI, land cover, and TDEP trends at an unprecedented scale across the CONUS that reveal specific patterns of stream loss associated with either modalities of watershed hysteresis (recovery) or one-way transition (new steady state) patterns. For the first time, we show that watershed retention of N can display unique hysteresis patterns, and that these patterns can be explained by the wealth of detailed mechanistic studies available for watersheds at different stages of response to changing N-deposition. In its present form, our conceptual model offers a valuable new insight into decade's worth of stream water data collection and highlights the value of stream water measurements as critical indicators of upstream watershed functionality.

6.0 Acknowledgements

This material is based upon work supported as part of the Watershed Function Scientific Focus Area funded by the U.S. Department of Energy, Office of Science, Office of Biological and Environmental Research under Award Number DE-AC02-05CH11231. We acknowledge the Total Deposition (TDEP) Science Committee of the National Atmospheric Deposition Program for their role in making the TDEP data and maps available at: http://nadp.slh.wisc.edu/committees/tdep/tdepmaps/. All analyzed data used for this study can be found in the following links and sources listed here: MODIS data are available at: http://dx.doi.org/10.3334/ORNLDAAC/1299. NLCD land cover and land cover change data are

available at: https://doi.org/10.5066/P937PN4Z. Elevation raster data are available at: https://www.hydroshare.org/resource/c18cef883695498c81acf9c4260d1e53/. Stream water N, C, and temperature data are available at: https://waterdata.usgs.gov/nwis. All watershed boundary shapefiles are available from the USGS Watershed Boundary Dataset (WBD) of the National Geospatial Program (https://usgs.gov/core-science-systems/ngp/national-hydrography). All gap-filled NWIS datasets that are merged with the CONUS scale NDVI, TDEP, Land Cover, and Elevation products that are produced within this study are freely available on ESS-DIVE (https://ess-dive.lbl.gov/) for free-public access and can be found directly through this DOI https://doi.org/10.15485/1647366. A description of these datasets can be found in Supplementary Text SA1. All station files for each water parameter are included in the data publication on ESS-DIVE.

7.0 Author Contributions

MN, HW, NB, SH contributed to experimental design. MN, DD, KW, and HW contributed to data collection and analysis. MN, DD, EW contributed to code design. MN, NB, TM, BA, EW, KW, CS, SH contributed to data interpretation. MN prepared the manuscript with contributions from all authors.

8.0 References

Aber, J. D., McDowell, W., Nadelhoffer, K., Magill, A., Berntson, G., Kamakea, M., et al. (1998). Nitrogen Saturation in Temperate Forest Ecosystems. *BioScience*, *48*(11), 921–934. https://doi.org/10.2307/1313296

Aber, J. D., Goodale, C. L., Ollinger, S. V., Smith, M.-L., Magill, A. H., Martin, M. E., et al. (2003). Is Nitrogen Deposition Altering the Nitrogen Status of Northeastern Forests? *BioScience*, *53*(4), 375. https://doi.org/10.1641/0006-3568(2003)053[0375:INDATN]2.0.CO;2

Argerich, A., Johnson, S. L., Sebestyen, S. D., Rhoades, C. C., Greathouse, E., Knoepp, J. D., et al. (2013). Trends in stream nitrogen concentrations for forested reference catchments across the USA. *Environmental Research Letters*, *8*(1), 014039. https://doi.org/10.1088/1748-9326/8/1/014039

Arora, B., Spycher, N. F., Steefel, C. I., Molins, S., Bill, M., Conrad, M. E., et al. (2016). Influence of hydrological, biogeochemical and temperature transients on subsurface carbon fluxes in a flood plain environment. *Biogeochemistry*, *127*(2–3), 367–396. https://doi.org/10.1007/s10533-016-0186-8

Arora, B., Burrus, M., Newcomer, M. E., Steefel, C. I., Carroll, R. W. H., Dwivedi, D., et al. (2020). Differential C-Q Analysis: A New Approach to Inferring Lateral Transport and Hydrologic Transients Within Multiple Reaches of a Mountainous Headwater Catchment. *Frontiers in Water*, *2*, 24. https://doi.org/10.3389/frwa.2020.00024

Ballard, T. C., Sinha, E., & Michalak, A. M. (2019). Long-Term Changes in Precipitation and Temperature Have Already Impacted Nitrogen Loading. *Environmental Science & Technology*, *53*(9), 5080–5090. https://doi.org/10.1021/acs.est.8b06898

Barnes, R. T., Butman, D. E., Wilson, H. F., & Raymond, P. A. (2018). Riverine Export of Aged Carbon Driven by Flow Path Depth and Residence Time. *Environmental Science & Technology*, *52*(3), 1028–1035. https://doi.org/10.1021/acs.est.7b04717

Basu, N. B., Destouni, G., Jawitz, J. W., Thompson, S. E., Loukinova, N. V., Darracq, A., et al. (2010). Nutrient loads exported from managed catchments reveal emergent biogeochemical stationarity: BIOGEOCHEMICAL STATIONARITY. *Geophysical Research Letters*, *37*(23), n/a-n/a. https://doi.org/10.1029/2010GL045168

Beaulieu, J. J., Tank, J. L., Hamilton, S. K., Wollheim, W. M., Hall, R. O., Mulholland, P. J., et al. (2011). Nitrous oxide emission from denitrification in stream and river networks. *Proceedings of the National Academy of Sciences*, *108*(1), 214–219. https://doi.org/10.1073/pnas.1011464108

Bellmore, R. A., Compton, J. E., Brooks, J. R., Fox, E. W., Hill, R. A., Sobota, D. J., et al. (2018). Nitrogen inputs drive nitrogen concentrations in U.S. streams and rivers during summer low flow conditions. *Science of The Total Environment*, *639*, 1349–1359. https://doi.org/10.1016/j.scitotenv.2018.05.008

Bernal, S., Hedin, L. O., Likens, G. E., Gerber, S., & Buso, D. C. (2012). Complex response of the forest nitrogen cycle to climate change. *Proceedings of the National Academy of Sciences*, *109*(9), 3406–3411. https://doi.org/10.1073/pnas.1121448109

Bernhardt, E. S., & Likens, G. E. (2004). Controls on periphyton biomass in heterotrophic streams. *Freshwater Biology*, *49*(1), 14–27. https://doi.org/10.1046/j.1365-2426.2003.01161.x

Bernhardt, E. S., Hall, Jr., R. O., & Likens, G. E. (2002). Whole-system Estimates of Nitrification and Nitrate Uptake in Streams of the Hubbard Brook Experimental Forest. *Ecosystems*, *5*(5), 419–430. https://doi.org/10.1007/s10021-002-0179-4

Bernhardt, E. S., Likens, G. E., Hall, R. O., Buso, D. C., Fisher, S. G., Burton, T. M., et al. (2005). Can't See the Forest for the Stream? In-stream Processing and Terrestrial

Nitrogen Exports. *BioScience*, *55*(3), 219. https://doi.org/10.1641/0006-3568(2005)055[0219:ACSTFF]2.0.CO;2

Bowden, R. D., Wurzbacher, S. J., Washko, S. E., Wind, L., Rice, A. M., Coble, A. E., et al. (2019). Long-term Nitrogen Addition Decreases Organic Matter Decomposition and Increases Forest Soil Carbon. *Soil Science Society of America Journal*, *83*(S1). https://doi.org/10.2136/sssaj2018.08.0293

Boyer, E. W., Goodale, C. L., Jaworski, N. A., & Howarth, R. W. (2002). Anthropogenic nitrogen sources and relationships to riverine nitrogen export in the northeastern U.S.A. *Biogeochemistry*, *57*(1), 137–169. https://doi.org/10.1023/A:1015709302073

Boyer, E. W., Howarth, R. W., Galloway, J. N., Dentener, F. J., Green, P. A., & Vörösmarty, C. J. (2006). Riverine nitrogen export from the continents to the coasts: RIVERINE NITROGEN EXPORT. *Global Biogeochemical Cycles*, *20*(1), n/a-n/a. https://doi.org/10.1029/2005GB002537

Cejudo, E., Hood, J. L., Schiff, S. L., & Aravena, R. O. (2018). Using the δ15N of submerged biomass for assessing changes in the nitrogen cycling in a river receiving wastewater treated effluent. *Ecological Indicators*, *95*, 645–653. https://doi.org/10.1016/j.ecolind.2018.08.013

Compton, J. E., Church, M. R., Larned, S. T., & Hogsett, W. E. (2003). Nitrogen Export from Forested Watersheds in the Oregon Coast Range: The Role of N 2 -fixing Red Alder. *Ecosystems*, *6*(8), 773–785. https://doi.org/10.1007/s10021-002-0207-4

Craine, J. M., Elmore, A. J., Wang, L., Aranibar, J., Bauters, M., Boeckx, P., et al. (2018). Isotopic evidence for oligotrophication of terrestrial ecosystems. *Nature Ecology & Evolution*, *2*(11), 1735–1744. https://doi.org/10.1038/s41559-018-0694-0

Crawford, J. T., Hinckley, E.-L. S., Litaor, M. I., Brahney, J., & Neff, J. C. (2019). Evidence for accelerated weathering and sulfate export in high alpine environments. *Environmental Research Letters, 14*(12), 124092. https://doi.org/10.1088/1748-9326/ab5d9c

Cusack, D. F., Silver, W. L., Torn, M. S., Burton, S. D., & Firestone, M. K. (2011). Changes in microbial community characteristics and soil organic matter with nitrogen additions in two tropical forests. *Ecology*, *92*(3), 621–632. https://doi.org/10.1890/10-0459.1

Driscoll, C. T., Driscoll, K. M., Roy, K. M., & Mitchell, M. J. (2003). Chemical Response of Lakes in the Adirondack Region of New York to Declines in Acidic Deposition. *Environmental Science & Technology*, *37*(10), 2036–2042. https://doi.org/10.1021/es020924h

Duncan, J. M., Groffman, P. M., & Band, L. E. (2013). Towards closing the watershed nitrogen budget: Spatial and temporal scaling of denitrification. *Journal of Geophysical Research: Biogeosciences*, *118*(3), 1105–1119. https://doi.org/10.1002/jgrg.20090

Duncan, J. M., Band, L. E., Groffman, P. M., & Bernhardt, E. S. (2015). Mechanisms driving the seasonality of catchment scale nitrate export: Evidence for riparian ecohydrologic controls: SEASONALITY OF CATCHMENT NITRATE EXPORT. *Water Resources Research*, *51*(6), 3982–3997. https://doi.org/10.1002/2015WR016937

Dwivedi, D., & Mohanty, B. (2016). Hot Spots and Persistence of Nitrate in Aquifers Across Scales. *Entropy*, *18*(1), 25. https://doi.org/10.3390/e18010025

EPA CASTNET. (2019). Clean Air Status and Trends Network (CASTNET) EPA CASTNET Total Wet and Dry Deposition. Retrieved from https://www.epa.gov/castnet

Eshleman, K. N., Sabo, R. D., & Kline, K. M. (2013). Surface Water Quality Is Improving due to Declining Atmospheric N Deposition. *Environmental Science & Technology*, *47*(21), 12193–12200. https://doi.org/10.1021/es4028748

Evans, C. D., Reynolds, B., Jenkins, A., Helliwell, R. C., Curtis, C. J., Goodale, C. L., et al. (2006). Evidence that Soil Carbon Pool Determines Susceptibility of Semi-Natural Ecosystems to Elevated Nitrogen Leaching. *Ecosystems*, *9*(3), 453–462. https://doi.org/10.1007/s10021-006-0051-z

Forbes, W. L., Mao, J., Ricciuto, D. M., Kao, S., Shi, X., Tavakoly, A. A., et al. (2019). Streamflow in the Columbia River Basin: Quantifying Changes Over the Period 1951-2008 and Determining the Drivers of Those Changes. *Water Resources Research*, *55*(8), 6640–6652. https://doi.org/10.1029/2018WR024256

Garayburu-Caruso, V. A., Stegen, J. C., Song, H.-S., Renteria, L., Wells, J., Garcia, W., et al. (2020). Carbon Limitation Leads to Thermodynamic Regulation of Aerobic Metabolism. *Environmental Science & Technology Letters*, acs.estlett.0c00258. https://doi.org/10.1021/acs.estlett.0c00258

Gilliam, F. S., Burns, D. A., Driscoll, C. T., Frey, S. D., Lovett, G. M., & Watmough, S. A. (2019). Decreased atmospheric nitrogen deposition in eastern North America: Predicted responses of forest ecosystems. *Environmental Pollution*, *244*, 560–574. https://doi.org/10.1016/j.envpol.2018.09.135

Goodale, C. L., Aber, J. D., & Vitousek, P. M. (2003). An Unexpected Nitrate Decline in New Hampshire Streams. *Ecosystems*, *6*(1), 0075–0086. https://doi.org/10.1007/s10021-002-0219-0

Goodale, C. L., Aber, J. D., Vitousek, P. M., & McDowell, W. H. (2005). Long-term Decreases in Stream Nitrate: Successional Causes Unlikely; Possible Links to DOC? *Ecosystems*, *8*(3), 334–337. https://doi.org/10.1007/s10021-003-0162-8

Grant, S. B., Azizian, M., Cook, P., Boano, F., & Rippy, M. A. (2018). Factoring stream turbulence into global assessments of nitrogen pollution. *Science*, *359*(6381), 1266–1269. https://doi.org/10.1126/science.aap8074

Groffman, P. M., Driscoll, C. T., Durán, J., Campbell, J. L., Christenson, L. M., Fahey, T. J., et al. (2018). Nitrogen oligotrophication in northern hardwood forests. *Biogeochemistry*, *141*(3), 523–539. https://doi.org/10.1007/s10533-018-0445-y

Guo, D., Lintern, A., Webb, J. A., Ryu, D., Liu, S., Bende-Michl, U., et al. (2019). Key Factors Affecting Temporal Variability in Stream Water Quality. *Water Resources Research*, *55*(1), 112–129. https://doi.org/10.1029/2018WR023370

Hale, R. L., Grimm, N. B., Vörösmarty, C. J., & Fekete, B. (2015). Nitrogen and phosphorus fluxes from watersheds of the northeast U.S. from 1930 to 2000: Role of anthropogenic nutrient inputs, infrastructure, and runoff. *Global Biogeochemical Cycles*, *29*(3), 341–356. https://doi.org/10.1002/2014GB004909

Halliday, S. J., Skeffington, R. A., Wade, A. J., Neal, C., Reynolds, B., Norris, D., & Kirchner, J. W. (2013). Upland streamwater nitrate dynamics across decadal to sub-daily timescales: a case study of Plynlimon, Wales. *Biogeosciences*, *10*(12), 8013–8038. https://doi.org/10.5194/bg-10-8013-2013

Heffernan, J. B., & Cohen, M. J. (2010). Direct and indirect coupling of primary production and diel nitrate dynamics in a subtropical spring-fed river. *Limnology and Oceanography*, *55*(2), 677–688. https://doi.org/10.4319/lo.2010.55.2.0677

Helsel, D. R., & Hirsch, R. M. (2002). *Statistical Methods in Water Resources*. U.S. Geological Survey. Retrieved from http://pubs.usgs.gov/twri/twri4a3/

Hirsch, R. M., & De Cicco, L. (2015). *User guide to Exploration and Graphics for RivEr Trends (EGRET) and dataRetrieval: R packages for hydrologic data (version 2.0, February 2015)*. Retrieved from https://dx.doi.org/10.3133/tm4A10

Hirsch, R. M., Moyer, D. L., & Archfield, S. A. (2010). Weighted Regressions on Time, Discharge, and Season (WRTDS), with an Application to Chesapeake Bay River Inputs. *JAWRA Journal of the American Water Resources Association*, *46*(5), 857–880. https://doi.org/10.1111/j.1752-1688.2010.00482.x

Hood, J. M., Benstead, J. P., Cross, W. F., Huryn, A. D., Johnson, P. W., Gíslason, G. M., et al. (2017). Increased resource use efficiency amplifies positive response of aquatic primary production to experimental warming. *Global Change Biology*. https://doi.org/10.1111/gcb.13912

Hubbard, S. S., Williams, K. H., Agarwal, D., Banfield, J., Beller, H., Bouskill, N., et al. (2018). The East River, Colorado, Watershed: A Mountainous Community Testbed for Improving Predictive Understanding of Multiscale Hydrological–Biogeochemical Dynamics. *Vadose Zone Journal*, *17*(1), 0. https://doi.org/10.2136/vzj2018.03.0061

Hungate, B. A., Lund, C. P., Pearson, H. L., & Chapin, Iii, F. S. (1997). Elevated CO2 and nutrient addition after soil N cycling and N trace gas fluxes with early season wet-up in a California annual grassland. *Biogeochemistry*, *37*(2), 89–109. https://doi.org/10.1023/A:1005747123463

Huntington, T. G. (2005). Can Nitrogen Sequestration Explain the Unexpected Nitrate Decline in New Hampshire Streams? *Ecosystems*, *8*(3), 331–333. https://doi.org/10.1007/s10021-004-0105-z

Hurst, H. E. (1951). Long-term Storage Capacity of Resevoirs. In *Transactions of the American Society of Civil Engineers* (Vol. 116, pp. 770–799). American Society of Civil Engineers.

Janssens, I. A., Dieleman, W., Luyssaert, S., Subke, J.-A., Reichstein, M., Ceulemans, R., et al. (2010). Reduction of forest soil respiration in response to nitrogen deposition. *Nature Geoscience*, *3*(5), 315–322. https://doi.org/10.1038/ngeo844

Jensen, A. M., Scanlon, T. M., & Riscassi, A. L. (2017). Emerging investigator series: the effect of wildfire on streamwater mercury and organic carbon in a forested watershed in the southeastern United States. *Environmental Science: Processes & Impacts*, *19*(12), 1505–1517. https://doi.org/10.1039/C7EM00419B

Kothawala, D. N., Watmough, S. A., Futter, M. N., Zhang, L., & Dillon, P. J. (2011). Stream Nitrate Responds Rapidly to Decreasing Nitrate Deposition. *Ecosystems*, *14*(2), 274–286. https://doi.org/10.1007/s10021-011-9422-1

Lawrence, G. B., Scanga, S. E., & Sabo, R. D. (2020). Recovery of Soils From Acidic Deposition May Exacerbate Nitrogen Export From Forested Watersheds. *Journal of Geophysical Research: Biogeosciences*, *125*(1). https://doi.org/10.1029/2019JG005036

Li, Y., Schichtel, B. A., Walker, J. T., Schwede, D. B., Chen, X., Lehmann, C. M. B., et al. (2016). Increasing importance of deposition of reduced nitrogen in the United States. *Proceedings of the National Academy of Sciences, 113*(21), 5874–5879. https://doi.org/10.1073/pnas.1525736113

Lovett, G. M., & Goodale, C. L. (2011). A New Conceptual Model of Nitrogen Saturation Based on Experimental Nitrogen Addition to an Oak Forest. *Ecosystems*, *14*(4), 615–631. https://doi.org/10.1007/s10021-011-9432-z

Lovett, G. M., Weathers, K. C., & Sobczak, W. V. (2000). Nitrogen Saturation and Retention in the Forested Watersheds of the Catskill Mountains, New York. *Ecological Applications*, *10*(1), 73–84. https://doi.org/10.1890/1051-0761(2000)010[0073:NSARIF]2.0.CO;2

Lovett, G. M., Goodale, C. L., Ollinger, S. V., Fuss, C. B., Ouimette, A. P., & Likens, G. E. (2018). Nutrient retention during ecosystem succession: a revised conceptual model. *Frontiers in Ecology and the Environment*, *16*(9), 532–538. https://doi.org/10.1002/fee.1949

Lucas, R. W., Klaminder, J., Futter, M. N., Bishop, K. H., Egnell, G., Laudon, H., & Högberg, P. (2011). A meta-analysis of the effects of nitrogen additions on base cations: Implications for plants, soils, and streams. *Forest Ecology and Management*, *262*(2), 95–104. https://doi.org/10.1016/j.foreco.2011.03.018

Lucas, R. W., Sponseller, R. A., Gundale, M. J., Stendahl, J., Fridman, J., Högberg, P., & Laudon, H. (2016). Long-term declines in stream and river inorganic nitrogen (N) export correspond to forest change. *Ecological Applications*, *26*(2), 545–556. https://doi.org/10.1890/14-2413

Maavara, T., Lauerwald, R., Laruelle, G. G., Akbarzadeh, Z., Bouskill, N. J., Van Cappellen, P., & Regnier, P. (2019). Nitrous oxide emissions from inland waters: Are IPCC estimates too high? *Global Change Biology*, *25*(2), 473–488. https://doi.org/10.1111/gcb.14504

Marinos, R. E., Campbell, J. L., Driscoll, C. T., Likens, G. E., McDowell, W. H., Rosi, E. J., et al. (2018). Give and Take: A Watershed Acid Rain Mitigation Experiment Increases

Baseflow Nitrogen Retention but Increases Stormflow Nitrogen Export. *Environmental Science & Technology*, *52*(22), 13155–13165. https://doi.org/10.1021/acs.est.8b03553

Maurer, E. P. (2016). CONUS digital elevation model of 1/16 degree grid cells. Retrieved from https://www.hydroshare.org/resource/c18cef883695498c81acf9c4260d1e53/

Maurer, E. P., Lettenmaier, D. P., & Mantua, N. J. (2004). Variability and potential sources of predictability of North American runoff. *Water Resources Research*, *40*(9). https://doi.org/10.1029/2003WR002789

Moatar, F., Abbott, B. W., Minaudo, C., Curie, F., & Pinay, G. (2017). Elemental properties, hydrology, and biology interact to shape concentration-discharge curves for carbon, nutrients, sediment, and major ions: SHAPES AND CAUSES OF C-Q RELATIONSHIPS. *Water Resources Research*, *53*(2), 1270–1287. https://doi.org/10.1002/2016WR019635

Monteith, D. T., Stoddard, J. L., Evans, C. D., de Wit, H. A., Forsius, M., Høgåsen, T., et al. (2007). Dissolved organic carbon trends resulting from changes in atmospheric deposition chemistry. *Nature*, *450*(7169), 537–540. https://doi.org/10.1038/nature06316

Moritz, S., Sardá, A., Bartz-Beielstein, T., Zaefferer, M., & Stork, J. (2015). Comparison of different Methods for Univariate Time Series Imputation in R. *ArXiv:1510.03924 [Cs, Stat]*. Retrieved from http://arxiv.org/abs/1510.03924

MRLC NLCD. (2020). NLCD Land Cover Change Index (CONUS) Multi-Resolution Land Characteristics (MRLC) consortium National Land Cover Database. Land Cover Change Index. Retrieved from https://www.mrlc.gov/data/nlcd-land-cover-change-index-conus

Mulholland, P. J., Helton, A. M., Poole, G. C., Hall, R. O., Hamilton, S. K., Peterson, B. J., et al. (2008). Stream denitrification across biomes and its response to anthropogenic nitrate loading. *Nature*, *452*(7184), 202–205. https://doi.org/10.1038/nature06686

Mulholland, P. J., Hall, R. O., Sobota, D. J., Dodds, W. K., Findlay, S. E. G., Grimm, N. B., et al. (2009). Nitrate removal in stream ecosystems measured by 15N addition experiments: Denitrification. *Limnology and Oceanography*, *54*(3), 666–680. https://doi.org/10.4319/lo.2009.54.3.0666

Murphy, J. C., & Sprague, L. A. (2019). Water-quality trends in US rivers: Exploring effects from streamflow trends and changes in watershed management. *Science of The Total Environment*, *656*, 645–658. https://doi.org/10.1016/j.scitotenv.2018.11.255

Murphy, S. F., Writer, J. H., McCleskey, R. B., & Martin, D. A. (2015). The role of precipitation type, intensity, and spatial distribution in source water quality after wildfire. *Environmental Research Letters*, *10*(8), 084007. https://doi.org/10.1088/1748-9326/10/8/084007

Musolff, A., Schmidt, C., Selle, B., & Fleckenstein, J. H. (2015). Catchment controls on solute export. *Advances in Water Resources*, *86*, 133–146. https://doi.org/10.1016/j.advwatres.2015.09.026

Musolff, A., Schmidt, C., Rode, M., Lischeid, G., Weise, S. M., & Fleckenstein, J. H. (2016). Groundwater head controls nitrate export from an agricultural lowland catchment. *Advances in Water Resources*, *96*, 95–107. https://doi.org/10.1016/j.advwatres.2016.07.003

Musolff, A., Selle, B., Büttner, O., Opitz, M., & Tittel, J. (2017). Unexpected release of phosphate and organic carbon to streams linked to declining nitrogen depositions. *Global Change Biology*, *23*(5), 1891–1901. https://doi.org/10.1111/gcb.13498

NADP. (2018). National Atmospheric Deposition Program (NRSP-3). NADP Program Office, Wisconsin State Laboratory of Hygiene, 465 Henry Mall, Madison, WI 53706. Retrieved October 24, 2018, from http://nadp.slh.wisc.edu/committees/tdep/tdepmaps/

Newcomer, M. E., Hubbard, S. S., Fleckenstein, J. H., Maier, U., Schmidt, C., Thullner, M., et al. (2018). Influence of Hydrological Perturbations and Riverbed Sediment Characteristics on Hyporheic Zone Respiration of CO_2 and N_2. *Journal of Geophysical Research: Biogeosciences*, *123*(3), 902–922. https://doi.org/10.1002/2017JG004090

Newcomer, M. E., Bouskill, N., Wainwright, H., Maavara, T., Arora, B., Woodburn, E., et al. (2020). Gap-filled water quality, Normalized Differenced Vegetation Index, total nitrogen (nitrate and ammonia) deposition, and land cover data trends for the Continental United States [Data set]. Environmental System Science Data Infrastructure for a Virtual Ecosystem; Watershed Function SFA. https://doi.org/10.15485/1647366

O’Donnell, J. A., Aiken, G. R., Kane, E. S., & Jones, J. B. (2010). Source water controls on the character and origin of dissolved organic matter in streams of the Yukon River basin, Alaska. *Journal of Geophysical Research*, *115*(G3). https://doi.org/10.1029/2009JG001153

Oelsner, G. P., & Stets, E. G. (2019). Recent trends in nutrient and sediment loading to coastal areas of the conterminous U.S.: Insights and global context. *Science of The Total Environment*, *654*, 1225–1240. https://doi.org/10.1016/j.scitotenv.2018.10.437

Oelsner, G. P., Sprague, L. A., Murphy, J. C., Zuellig, R. E., Johnson, H. M., Ryberg, K. R., et al. (2017). *Water-quality trends in the Nation's rivers and streams, 1972–2012—Data preparation, statistical methods, and trend results (ver. 2.0, October 2017)* (Scientific Investigations Report No. U.S. Geological Survey Scientific Investigations Report 2017–5006) (p. 136). U.S. Geological Survey. Retrieved from https://doi.org/10.3133/sir20175006

Pardo, L. H., Fenn, M. E., Goodale, C. L., Geiser, L. H., Driscoll, C. T., Allen, E. B., et al. (2011). Effects of nitrogen deposition and empirical nitrogen critical loads for ecoregions of the United States. *Ecological Applications*, *21*(8), 3049–3082. https://doi.org/10.1890/10-2341.1

Pinder, R. W., Davidson, E. A., Goodale, C. L., Greaver, T. L., Herrick, J. D., & Liu, L. (2012). Climate change impacts of US reactive nitrogen. *Proceedings of the National Academy of Sciences*, *109*(20), 7671–7675. https://doi.org/10.1073/pnas.1114243109

Quilbé, R., Rousseau, A. N., Duchemin, M., Poulin, A., Gangbazo, G., & Villeneuve, J.-P. (2006). Selecting a calculation method to estimate sediment and nutrient loads in streams: Application to the Beaurivage River (Québec, Canada). *Journal of Hydrology*, *326*(1–4), 295–310. https://doi.org/10.1016/j.jhydrol.2005.11.008

R Core Team. (2020). R: A language and environment for statistical computing. Retrieved from http://www.R-project.org/.

Read, E. K., Carr, L., De Cicco, L., Dugan, H. A., Hanson, P. C., Hart, J. A., et al. (2017). Water quality data for national-scale aquatic research: The Water Quality Portal. *Water Resources Research*, *53*(2), 1735–1745. https://doi.org/10.1002/2016WR019993

Renwick, W. H., Vanni, M. J., Fisher, T. J., & Morris, E. L. (2018). Stream Nitrogen, Phosphorus, and Sediment Concentrations Show Contrasting Long-term Trends Associated with Agricultural Change. *Journal of Environmental Quality*, *47*(6), 1513–1521. https://doi.org/10.2134/jeq2018.04.0162

Rhoades, C. C., Hubbard, R. M., & Elder, K. (2017). A Decade of Streamwater Nitrogen and Forest Dynamics after a Mountain Pine Beetle Outbreak at the Fraser Experimental Forest, Colorado. *Ecosystems*, *20*(2), 380–392. https://doi.org/10.1007/s10021-016-0027-6

Rhoades, C. C., Chow, A. T., Covino, T. P., Fegel, T. S., Pierson, D. N., & Rhea, A. E. (2018). The Legacy of a Severe Wildfire on Stream Nitrogen and Carbon in Headwater Catchments. *Ecosystems*. https://doi.org/10.1007/s10021-018-0293-6

Rice, J., & Westerhoff, P. (2017). High levels of endocrine pollutants in US streams during low flow due to insufficient wastewater dilution. *Nature Geoscience*, *10*(8), 587–591. https://doi.org/10.1038/ngeo2984

Rogers, D. B., Newcomer, M. E., Raberg, J. H., Dwivedi, D., Steefel, C., Bouskill, N., et al. (2021). Modeling the Impact of Riparian Hollows on River Corridor Nitrogen Exports. *Frontiers in Water*, *3*, 590314. https://doi.org/10.3389/frwa.2021.590314

SanClements, M. D., Fernandez, I. J., Lee, R. H., Roberti, J. A., Adams, M. B., Rue, G. A., & McKnight, D. M. (2018). Long-Term Experimental Acidification Drives Watershed Scale Shift in Dissolved Organic Matter Composition and Flux. *Environmental Science & Technology*, *52*(5), 2649–2657. https://doi.org/10.1021/acs.est.7b04499

Schwede, D. B., & Lear, G. G. (2014). A novel hybrid approach for estimating total deposition in the United States. *Atmospheric Environment*, *92*, 207–220. https://doi.org/10.1016/j.atmosenv.2014.04.008

Schwesig, D., Kalbitz, K., & Matzner, E. (2003). Mineralization of dissolved organic carbon in mineral soil solution of two forest soils. *Journal of Plant Nutrition and Soil Science*, *166*(5), 585–593. https://doi.org/10.1002/jpln.200321103

Seaber, P. R., Kapinos, F. P., & Knapp, G. L. (1987). *Hydrologic Unit Maps* (USGS Water Supply Paper No. Water-Supply Paper 2294) (p. 63). U.S. Geological Survey. Retrieved from https://water.usgs.gov/GIS/huc.html

Seitzinger, S., Harrison, J. A., Böhlke, J. K., Bouwman, A. F., Lowrance, R., Peterson, B., et al. (2006). Denitrifcation Across Landscapes and Watersheds: A Synthesis. *Ecological Applications*, *16*(6), 2064–2090. https://doi.org/10.1890/1051-0761(2006)016[2064:DALAWA]2.0.CO;2

Shoda, M. E., Sprague, L. A., Murphy, J. C., & Riskin, M. L. (2019). Water-quality trends in U.S. rivers, 2002 to 2012: Relations to levels of concern. *Science of The Total Environment*, *650*, 2314–2324. https://doi.org/10.1016/j.scitotenv.2018.09.377

Shultz, M., Pellerin, B., Aiken, G., Martin, J., & Raymond, P. (2018). High Frequency Data Exposes Nonlinear Seasonal Controls on Dissolved Organic Matter in a Large Watershed. *Environmental Science & Technology*, *52*(10), 5644–5652. https://doi.org/10.1021/acs.est.7b04579

Sinha, E., & Michalak, A. M. (2016). Precipitation Dominates Interannual Variability of Riverine Nitrogen Loading across the Continental United States. *Environmental Science & Technology*, *50*(23), 12874–12884. https://doi.org/10.1021/acs.est.6b04455

Smith, R. A., Alexander, R. B., & Wolman, M. G. (1987). Water-Quality Trends in the Nation's Rivers. *Science*, *235*(4796), 1607–1615. https://doi.org/10.1126/science.235.4796.1607

Spruce, J. P., Gasser, G. E., & Hargrove, W. W. (2016). MODIS NDVI Data, Smoothed and Gap-filled, for the Conterminous US: 2000-2015. ORNL Distributed Active Archive Center. https://doi.org/10.3334/ORNLDAAC/1299

Stegen, J. C., Johnson, T., Fredrickson, J. K., Wilkins, M. J., Konopka, A. E., Nelson, W. C., et al. (2018). Influences of organic carbon speciation on hyporheic corridor biogeochemistry and microbial ecology. *Nature Communications*, *9*(1), 585. https://doi.org/10.1038/s41467-018-02922-9

Stets, E. G., Sprague, L. A., Oelsner, G. P., Johnson, H. M., Murphy, J. C., Ryberg, K., et al. (2020). Landscape Drivers of Dynamic Change in Water Quality of U.S. Rivers. *Environmental Science & Technology*, *54*(7), 4336–4343. https://doi.org/10.1021/acs.est.9b05344

Stoddard, J. L. (1994). Long-Term Changes in Watershed Retention of Nitrogen: Its Causes and Aquatic Consequences. In L. A. Baker (Ed.), *Environmental Chemistry of Lakes and Reservoirs* (Vol. 237, pp. 223–284). Washington, DC: American Chemical Society. https://doi.org/10.1021/ba-1994-0237.ch008

Stoddard, J. L., Jeffries, D. S., Lükewille, A., Clair, T. A., Dillon, P. J., Driscoll, C. T., et al. (1999). Regional trends in aquatic recovery from acidification in North America and Europe. *Nature*, *401*(6753), 575–578. https://doi.org/10.1038/44114

Stoddard, J. L., Van Sickle, J., Herlihy, A. T., Brahney, J., Paulsen, S., Peck, D. V., et al. (2016). Continental-Scale Increase in Lake and Stream Phosphorus: Are Oligotrophic Systems

Disappearing in the United States? *Environmental Science & Technology*, *50*(7), 3409–3415. https://doi.org/10.1021/acs.est.5b05950

Strauss, E. A., Richardson, W. B., Bartsch, L. A., Cavanaugh, J. C., Bruesewitz, D. A., Imker, H., et al. (2004). Nitrification in the Upper Mississippi River: patterns, controls, and contribution to the NO_3^- budget. *Journal of the North American Benthological Society*, *23*(1), 1–14. https://doi.org/10.1899/0887-3593(2004)023<0001:NITUMR>2.0.CO;2

Sudduth, E. B., Perakis, S. S., & Bernhardt, E. S. (2013). Nitrate in watersheds: Straight from soils to streams. *Journal of Geophysical Research: Biogeosciences*, *118*(1), 291–302. https://doi.org/10.1002/jgrg.20030

Terrer, C., Vicca, S., Stocker, B. D., Hungate, B. A., Phillips, R. P., Reich, P. B., et al. (2018). Ecosystem responses to elevated CO_2 governed by plant-soil interactions and the cost of nitrogen acquisition. *New Phytologist*, *217*(2), 507–522. https://doi.org/10.1111/nph.14872

Van Breemen, N., Boyer, E. W., Goodale, C. L., Jaworski, N. A., Paustian, K., Seitzinger, S. P., et al. (2002). Where Did All the Nitrogen Go? Fate of Nitrogen Inputs to Large Watersheds in the Northeastern U.S.A. *Biogeochemistry*, *57/58*, 267–293.

Van Meter, K. J., & Basu, N. B. (2015). Catchment Legacies and Time Lags: A Parsimonious Watershed Model to Predict the Effects of Legacy Storage on Nitrogen Export. *PLOS ONE*, *10*(5), e0125971. https://doi.org/10.1371/journal.pone.0125971

Van Meter, K. J., & Basu, N. B. (2017). Time lags in watershed-scale nutrient transport: an exploration of dominant controls. *Environmental Research Letters*, *12*(8), 084017. https://doi.org/10.1088/1748-9326/aa7bf4

Van Meter, K. J., Basu, N. B., Veenstra, J. J., & Burras, C. L. (2016). The nitrogen legacy: emerging evidence of nitrogen accumulation in anthropogenic landscapes. *Environmental Research Letters*, *11*(3), 035014. https://doi.org/10.1088/1748-9326/11/3/035014

Van Meter, K. J., Basu, N. B., & Van Cappellen, P. (2017). Two centuries of nitrogen dynamics: Legacy sources and sinks in the Mississippi and Susquehanna River Basins: Two centuries of nitrogen dynamics. *Global Biogeochemical Cycles*, *31*(1), 2–23. https://doi.org/10.1002/2016GB005498

Vitousek, P. M., & Reiners, W. A. (1975). Ecosystem Succession and Nutrient Retention: A Hypothesis. *BioScience*, *25*(6), 376–381. https://doi.org/10.2307/1297148

Vuorenmaa, J., Augustaitis, A., Beudert, B., Bochenek, W., Clarke, N., de Wit, H. A., et al. (2018). Long-term changes (1990–2015) in the atmospheric deposition and runoff water chemistry of sulphate, inorganic nitrogen and acidity for forested catchments in Europe in relation to changes in emissions and hydrometeorological conditions. *Science of The Total Environment*, *625*, 1129–1145. https://doi.org/10.1016/j.scitotenv.2017.12.245

Wasserstein, R. L., & Lazar, N. A. (2016). The ASA Statement on *p* -Values: Context, Process, and Purpose. *The American Statistician*, *70*(2), 129–133. https://doi.org/10.1080/00031305.2016.1154108

Yanai, R. D., Vadeboncoeur, M. A., Hamburg, S. P., Arthur, M. A., Fuss, C. B., Groffman, P. M., et al. (2013). From Missing Source to Missing Sink: Long-Term Changes in the Nitrogen Budget of a Northern Hardwood Forest. *Environmental Science & Technology*, *47*(20), 11440–11448. https://doi.org/10.1021/es4025723

Yang, L., Jin, S., Danielson, P., Homer, C., Gass, L., Bender, S. M., et al. (2018). A new generation of the United States National Land Cover Database: Requirements, research priorities, design, and implementation strategies. *ISPRS Journal of Photogrammetry and Remote Sensing*, *146*, 108–123. https://doi.org/10.1016/j.isprsjprs.2018.09.006

Zarnetske, J. P., Bouda, M., Abbott, B. W., Saiers, J., & Raymond, P. A. (2018). Generality of Hydrologic Transport Limitation of Watershed Organic Carbon Flux Across Ecoregions of the United States. *Geophysical Research Letters*, *45*(21), 11,702-11,711. https://doi.org/10.1029/2018GL080005